Title

Temporalis attachment area as a proxy for feeding ecology in toothed whales (Artiodactyla: Odontoceti)

Journal

PaleoBios, 41(3)

ISSN

0031-0298

Authors

Xiong, Doua C
Beatty, Brian L
Churchill, Morgan

Publication Date

2024

DOI

10.5070/P941361509

PaleoBios

OFFICIAL PUBLICATION OF THE UNIVERSITY OF CALIFORNIA MUSEUM OF PALEONTOLOGY

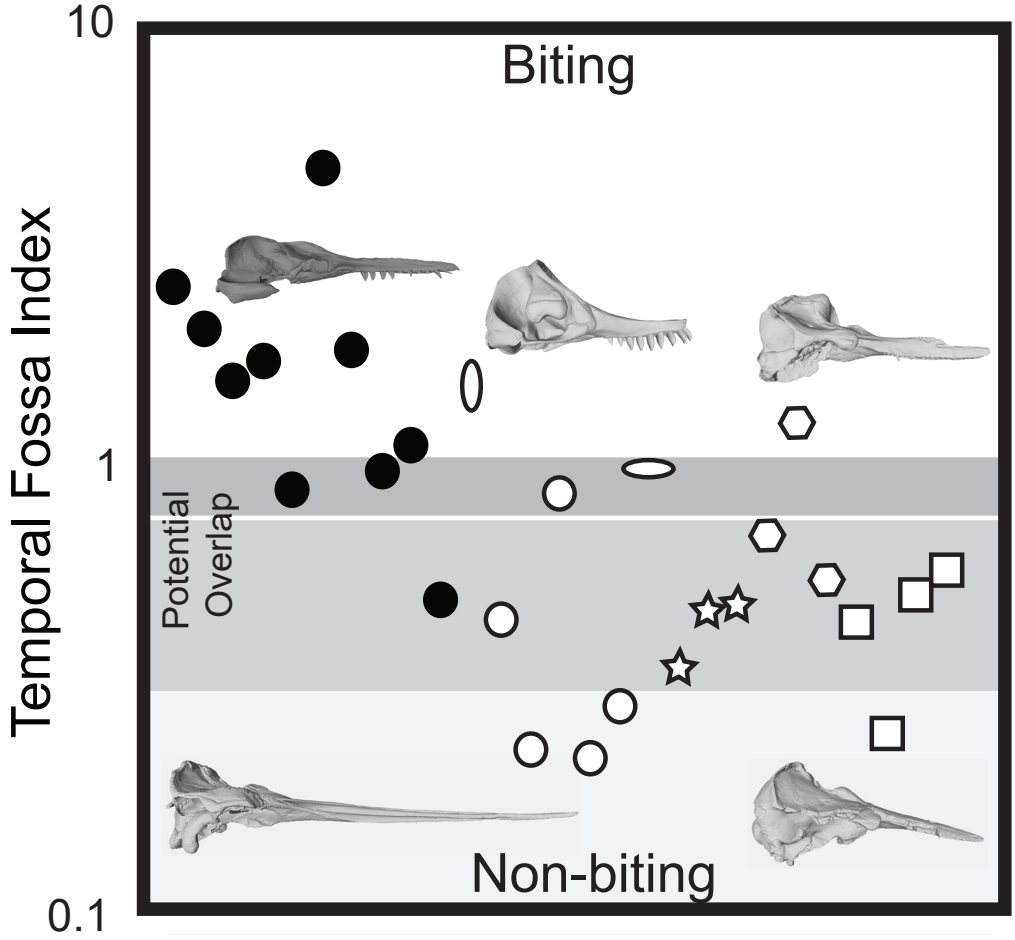

Doua C. XIONG, Brian L. BEATTY, and Morgan CHURCHILL (2024). Temporalis attachment area as a proxy for feeding ecology in toothed whales (Artiodactyla: Odontoceti)

Cover: Illustration of inferred prey capture and processing behavior in extinct odontocete whales, using the temporal fossa index (TFI)

Citation: . Xiong, D. C., B. L. Beatty, and M. Churchill. 2024. Temporalis attachment area as a proxy for feeding ecology in toothed whales (Artiodactyla: Odontoceti). *PaleoBios* 41(3): 1-29.

DOI: https://doi.org/10.5070/P941361509

Temporalis attachment area as a proxy for feeding ecology in toothed whales (Artiodactyla: Odontoceti)

Doua C. Xiong[1,2], Brian L. Beatty[3], and Morgan Churchill[1*]

[1] Department of Biology, University of Wisconsin Oshkosh, Oshkosh WI 54901
[2] University of Wisconsin School of Medicine and Public Health,
Madison WI 53705; douaxiongc@gmail.com
[3] Department of Anatomy, College of Osteopathic Medicine, New York Institute of Technology,
Old Westbury NY 11568, USA; bbeatty@nyit.edu
[*] corresponding author; churchim@uwosh.edu

The temporalis is an important muscle used in biting and mastication, and whose morphology is strongly influenced by feeding ecology. Although the anatomy of this muscle and its relation to feeding function are well-studied in terrestrial mammals, few studies have examined its variation in whales. Our study focuses on quantifying the area of attachment for the temporalis muscle within the temporal fossa, calculating two metrics of comparison: A temporal fossa index (TFI) which is a size corrected measure of temporalis muscle attachment area, and a corrected temporal fossa index (CTFI), which also corrects for cranial telescoping. We calculated TFI and CTFI scores for 72 species of extant odontocetes as well as 37 species of extinct whale, including archaeocetes and toothed mysticetes. We statistically tested for differences related to diet and prey capture method using ANOVA. We then performed ancestral character state reconstruction (ACSR) for both metrics.

We found no significant differences in TFI scores for diet, however both grip-and-tear as well as snap feeding taxa had significantly larger TFI scores than suction or ram feeding odontocetes. The ACSR found major decreases in TFI at the base of the Neoceti, Odontoceti, and just prior to the evolution of the crown group, relating to the gradual loss of mastication. When we corrected for telescoping, CTFI scores increase within mysticetes and stem odontocetes, before decreasing again within crown odontocetes. This suggests that as telescoping increased, some compensation was needed to account for the reduced intertemporal region. We find evidence of macropredatory behavior for *Basilosaurus*, *Coronodon*, *Ankylorhiza*, *Livyatan*, and possibly *Atocetus*. Hyper-longirostrine taxa such as eurhinodelphinids possess unusually low TFI scores, as does the bizarre prognathous porpoise *Semirostrum*, highlighting their unique feeding styles. Our study reveals a complex interplay between the reduction in mastication, increase in cranial telescoping, and prey capture specialization. It also introduces a useful and simple metric which can be used to infer feeding ecology in extinct whales.

Keywords: Odontocetes, feeding ecology, temporalis, prey capture, whale evolution

Citation: Xiong, D. C., B. L. Beatty, and M. Churchill. 2024. Temporalis attachment area as a proxy for feeding ecology in toothed whales (Artiodactyla: Odontoceti). *PaleoBios* 41(3): 1-29.
DOI: https://doi.org/10.5070/P941361509

INTRODUCTION

Toothed whales (Odontoceti) consist of ~78 species found throughout the world's oceans and several major freshwater river systems, and are distinguished from mysticetes, the other major group of living whales, by the ability to echolocate, lack of baleen, and extreme retrograde cranial telescoping. The numerical diversity of this clade is matched by the ecological diversity, which includes deep-diving squid hunting sperm and beaked whales, gharial-like freshwater river dolphins, and macropredatory killer whales, alongside an assortment of more generalized fish and squid-eating dolphins that lack the specialized feeding adaptations of the former species.

The differences in ecology between different groups of odontocetes have resulted in differences in prey capture and processing strategies. These strategies can largely be divided into three major methods: suction, raptorial, and grip-and-tear (Berta and Lanzetti 2020, Galatius et al. 2020, Kienle et al. 2017, Werth 2000). Suction feeding occurs when whales quickly retract their tongue creating negative pressure inside the buccal cavity, drawing in prey like squid, shrimp, and benthic invertebrates (Berta and Lanzetti 2020, Kane and Marshall 2009, Werth 2000). Specialized suction feeders such as belugas and pilot whales have short rostra, blunt heads, and reduced dentition allowing them to efficiently siphon prey (Heyning and Mead 1996, Johnston and Berta 2011, Werth 2000, 2006). Suction-feeding specialists can be found in nearly every marine family of odontocete and have evolved multiple times within Odontoceti (Boessenecker et al. 2017).

Raptorial feeding works by grasping prey with pincer-like jaws and fast lateral movements of the head (snapping) or with an explosive forward movement of the body (ram-feeding; (Bloodworth and Marshall 2005, Hocking et al. 2017b, McCurry et al. 2017a, Werth 2000). The sharp teeth projecting from the rostrum and jaws enable raptorial feeders to maintain a grip on slippery prey (Werth 2000). Snap-feeding is performed by river dolphins belonging to four living odontocete families, Platanistidae, Lipotidae, Pontoporiidae, and Iniidae (McCurry et al. 2017a, Werth 2000). These dolphins have flexible necks and elongated jaws bearing hundreds of teeth able to quickly snag fast moving prey such as fish (McCurry et al. 2017a, Werth 2000). Ram-feeding is used by most other odontocetes, especially within the family Delphinidae. These taxa have fusiform bodies, elongate rostra, and small conical teeth (Werth 2000).

Grip-and-tear feeding is performed by only two taxa, the killer whale (*Orcinus)* and false killer whale (*Pseudorca*; Galatius et al. 2020). Grip-and-tear feeders have blunt heads and large, sharp interlocking teeth (Berta and Lanzetti 2020, McCurry et al. 2017a, Werth 2000). These taxa often capture large prey items which are too large to swallow intact, the more common mode of ingestion in whales. Instead, they use their powerful jaws and twisting body motions to dismember the prey into smaller pieces which can be swallowed whole, often with the aid of other individuals (Pitman and Durban 2012).

These different diets and prey capture strategies are likely to influence the musculature of the whale, especially the temporalis muscle, a jaw elevator muscle active during mastication that contributes to the bite force of an animal (Herrel et al. 2008, Turnbull 1970). The temporalis muscle in odontocete whales such as dolphins originates from the temporal fossa of the cranium and proximally attaches to the coronoid process of the mandible (Cozzi et al. 2017). As the temporalis muscle contracts, the jaw closes and bite force is generated. Although the relationship between temporalis size and bite force has been studied in a wide variety of organisms (Mioche et al. 1999, Fabre et al. 2017, Santana et al. 2010, Meyers et al. 2017), few studies have looked at odontocetes specifically, although studies have called for further investigation (Werth and Beatty 2023). Prior studies have correlated increasing temporal fossa size with increasing prey size (Galatius et al. 2020, Perrin 1975), while other studies have quantified the size of the temporalis in specific species of extinct whale to estimate bite force (Peri et al. 2022, Snively et al. 2015). Boessenecker and Geisler (2023) examined the evolution of the temporal fossa in xenorophids, using a simple measure of temporal fossa length vs. bizygomatic width. They found that overall archaeocetes as well as stem odontocetes and stem mysticetes had proportionally larger temporal fossae than crown taxa, although they did not take in account factors such as cranial telescoping variation or height of the fossa in their analysis.

Our study seeks to quantify the area of superior attachment for the temporalis muscle, in a wide variety of extant and extinct odontocete whale taxa. Using these data as a proxy for the size of the muscle, we will trace the evolution of the temporalis muscle through time and test for relationships between size of the muscle and diet and prey capture technique. We predict that grip-and-tear feeders as well as snap feeders will possess large areas of attachment, as biting is important in their methods of feeding, while the temporalis will be significantly reduced in size within suction-feeding

specialists, where biting doesn't play a significant role in prey capture. We will then use these data to infer the foraging ecology of extinct whales.

MATERIALS AND METHODS

Data Collection

Measurements were collected from 209 complete adult skulls belonging to 72 extant species of odontocete whales (Appendix 1; Supplemental Material), representing at least one specimen from every living family. We assessed maturity of individuals sampled using suture closure and skull size, with juveniles whenever possible excluded from our study. In addition to the extant taxa, we also included 43 fossil skulls from 37 species of extinct taxa. Extinct species sampled included six archaeocetes, four toothed mysticetes, ten stem odontocetes (including three xenorophids), five platanistoids, one physeteroid, one ziphiid, three kentriodontids, three inioids, and four delphinoids.

We collected measurements using STL files produced from 3D scans of whale skulls. Scan data was initially collected using a Handyscan Creaform 700 3D laser scanner or an Artec Space Spider white light scanner. We downloaded additional STL files for extinct taxa missing from our dataset from the website Phenome10k (www.phenome10k.org) or they were provided by museums. We collected five separate measurements in Artec Studio 13 using the linear measure tool (Fig. 1). Measurements we recorded included height of the temporal fossa (TFH) and the length of the temporal fossa (TFL) for the right and left sides of each skull separately. We measured the height of the temporal fossa vertically on the lateral wall of the braincase from the dorsal portion of the temporal crest to the level of the subtemporal crest. We recorded this measurement just anterior to the squamosal fossa, and when possible, the measurement recorded is the maximum possible distance between the subtemporal and temporal crests. We recorded temporal fossa length as the horizontal distance from the approximate midpoint of the parietal-frontal suture on the braincase to the posterior portion of the temporal crest. Additionally, we collected data on maximum occipital condyle breath (OCB) as a proxy for body size. We made each measurement three times, then averaged. We then divided the average TFH and average TFL by the average OCB to standardize measurements and to remove the influence of varying body size between different whale species. We then used these size-corrected measurements to calculate the temporal fossa index (TFI). The TFI represents the approximate size of the area of attachment for the temporalis muscle in the temporal fossa and we calculated this value by multiplying the size-corrected TFH by the size-corrected TFL. While the potential area of attachment for the temporalis muscle is not exactly rectangular in shape, it is similar enough to a rectangle or square that the TFI provides useful relative measure of the area of attachment.

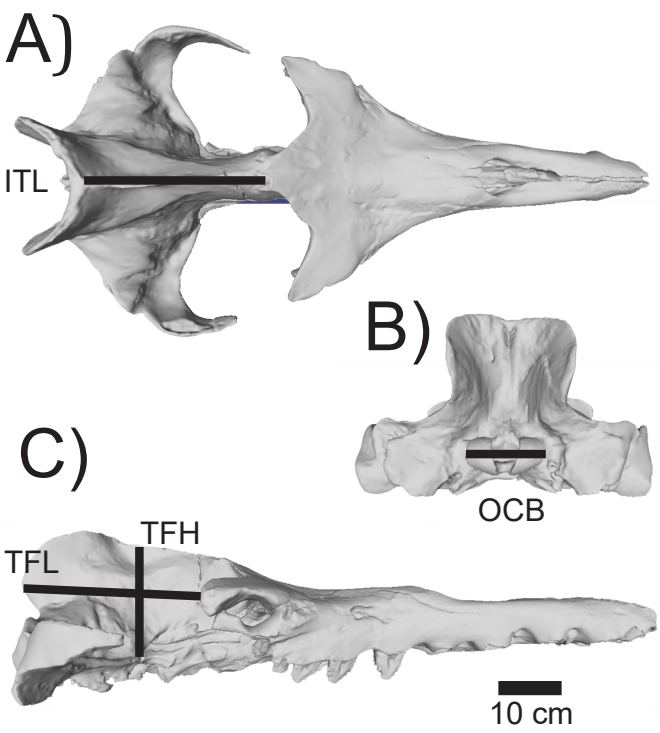

Figure 1. Cranial measurements used in analyses carried out in this study, illustrated on a skull of *Basilosaurus isis* (SMNS 11787), in dorsal (A), posterior (B), and lateral (C) views. ITL = length of intertemporal region; OCB = occipital condyle breadth; TFH = height of temporal fossa; TFL = length of temporal fossa. Scale bar=10 cm.

All crown odontocetes have an equivalent degree of cranial telescoping (Churchill et al. 2018a), with retrograde movement of the facial bone elements such as the frontal, maxilla, and premaxilla, and prograde movement of the supraoccipital. This results in no exposure of the parietal in dorsal view, and a temporal fossa of comparable shape. However, taxa outside the crown group often have lesser degrees of cranial telescoping (Churchill et al. 2018a), which results in a longer intertemporal region and larger potential TFI scores. If not taken in account, this would reduce comparability of archaeocetes, toothed mysticetes, and stem odontocetes with modern whales. To accommodate differences in telescoping between taxa, we measured the length of the intertemporal region

(ITL), from the apex of the supraoccipital shield to the frontal-parietal suture along the midline of the skull. In crown odontocetes, the supraoccipital and frontal are in contact, and so a measurement value of 0 was recorded for these taxa. We divided length of the intertemporal region by occipital condyle breadth to remove size variation, treating the resulting value as a proxy for degree of telescoping. To correct for telescoping in the TFI data, we performed a linear regression of telescoping scores vs TFI scores. We then used the resulting linear equation produced to estimate the TFI score based on a given value for telescoping. After this, we subtracted the estimated TFI score from the known TFI score; the resulting value was treated as the Corrected Temporal Fossa Index (CTFI) score, with negative values indicating a TFI lower than expected for a given degree of telescoping, and a positive score indicating a higher TFI score than expected.

Cranial Asymmetry and TFI

Odontocete skulls are known to be highly asymmetrical, especially the nasofacial region (Coombs et al. 2020, Ness 1967). While asymmetry is not readily apparent in the squamosal and lateral walls of the braincase, we were concerned that asymmetry in other parts of the skull may have influenced this region as well and could bias comparisons of TFI between specimens and taxa. To assess whether there was asymmetry in the area of attachment for the temporalis muscle between the right and left sides of the skull, paired t-tests were performed to assess if there was any difference in uncorrected TFI in the skull between the right and left temporal fossa. If we detected no significant asymmetry (P-value > 0.05), TFI would be averaged between the left and right side. If we detected asymmetry, the left and right temporal fossa area were treated as different data sets for further analysis, with comparison only being made between TFI derived from the left side. Tests for the influence of asymmetry on TFI for extant odontocete taxa were performed for the entire suborder (Odontoceti), as well as for smaller clades within the suborder, including Physeteroidea, Ziphiidae, Inioidea, and Delphinoidea, using the phylogeny of McGowen et al. (2020) for placement of taxa into different clades. We included *Platanista* within the analysis that included all odontocetes, but with its limited extant diversity and small sample size, was not included in a separate clade specific analysis. We also examined asymmetry within the most specious and diverse living odontocete clade, Delphinoidea, assessing asymmetry, separately for Monodontidae, Phocoenidae, and Delphinidae. Furthermore, we also assessed asymmetry within Delphinidae, by comparing asymmetry among the major subfamilies, following the taxonomy suggested by McGowen et al. (2020). We excluded three taxa from these subfamily level analyses this analysis, including *Lagenorhynchus albirostris*, *Leucopleurus acutus*, and *Orcinus orca*. All three species represent stem taxa that do not belong to any of the major subfamilies (McGowen 2011, McGowen et al. 2020), with limited diversity and sampling in this study. Overall, we examined three subfamilies for asymmetry: Lissodelphinae (*Sagmatias, Cephalorhynchus,* and *Lissodelphis*), Globicephalinae (*Steno*, *Orcaella, Grampus*, *Pepenocephala, Feresa, Pseudorca,* and *Globicephala*), and Delphininae (*Sotalia*, *Sousa, Tursiops, Lagenodelphis, Stenella,* and *Delphinus*).

Variation in TFI Scores between Different Taxonomic Groups

After testing for asymmetry, We performed Kruskal-Wallis tests and Wilcoxon rank sum tests with Bonferroni adjustments to look for statistical differences in TFI scores related to taxonomic classification. We performed two separate analyses. In both analyses, all extinct and extant taxa were included together. For the first analysis, we focused on the uncorrected TFI scores. We separated all whales into nine major groups, four of which only included extinct taxa and two of which represented paraphyletic assemblages of taxa. The groups consisting solely of extinct taxa included the Archaeoceti, a paraphyletic assemblage of stem whales (*Ambulocetus*, *Aegyptocetus*, *Basilosaurus*, *Cynthiacetus*, *Zygorhiza*, and *Dorudon*); Mysticeti, consisting of only of toothed members of this clade (*Coronodon*, *Janjucetus*, *Aetiocetus*, and *Fucaia*), Xenorophidae (*Albertocetus*, *Cotylocara*, and *Xenorophus*), and finally a group comprising extinct stem odontocetes, taxa that diverged after Xenorophidae but before the origin of crown Odontoceti, following Churchill et al. (2018a) and Boessenecker et al. (2020). This latter group included *Agorophius*, *Ankylorhiza*, *Waipatia*, *Prosqualodon*, *Eosqualodon*, and *Argyrocetus*. We also specifically tested for significant differences within just the crown group, focusing on just extant species.

We classified crown Odontoceti into five major superfamilies: Physeteroidea, Platanistoidea (including both Eurhinodelphinidae and Platanistidae), Ziphioidea, Inioidea, and Delphinoidea. We treated three extinct taxa (*Atocetus*, *Kentriodon*, and *Lamprolithax*) belonging to the paraphyletic Kentriodontidae as delphinoids for this analysis, as they are often recovered to be closely related to this clade (Guo and Kohno 2021). Classification of taxa follows Coombs et al. (2022). For the second analysis,

the same taxa and categories from the first analysis were used, but analyses were made using CTFI scores instead of the raw TFI scores.

Ancestral Character State Analysis (ACSR)

To reconstruct how TFI and CTFI, and consequently the size of the temporal fossa, changed over time, we performed an ancestral character state reconstruction (ACSR) to map TFI and CTFI scores onto a time-scaled phylogeny of whales. The phylogeny is a modified version of the metatree from Lloyd and Slater (2021), with taxa not examined in our study pruned from the tree. We also have modified the phylogenetic relationships within the family Delphinidae to reflect the results of McGowen et al. (2020). One extinct taxon was included in our study that was not present in Lloyd and Slater (2021), *Eosqualodon* sp. *Eosqualodon* has not appeared in any recent robust study of odontocete phylogeny, however it has traditionally been considered closely related to *Squalodon* (Marx et al. 2016b). We used the position of *Squalodon* in Lloyd and Slater (2021) to infer the position of *Eosqualodon* for our tree.

We generated branch lengths for the tree by time scaling the phylogeny using the R package Paleotree (Bapst 2012), using first (FAD) and last (LAD) appearance data from Churchill and Baltz (2021). For those taxa not included in Churchill and Baltz (2021), FAD and LAD data was collected from the Paleobiology Database (www.paleobiodb.org). These data are included within the online Supplemental Material.

Prior to the ancestral character state analysis, we tested for phylogenetic signal in TFI and CTFI scores using Pagel's λ (Pagel 1999). This step is prerequisite for ancestral character state reconstruction, because if there were no phylogenetic signal in the data it would be pointless to map it onto a tree. We calculated phylogenetic signal using the methods of Churchill and Baltz (2021) using the APE (Paradis et al. 2004) and GEIGER (Harmon et al. 2010) packages.

If we detected strong phylogenetic signal, ACSR using the R package Phytools (Revell 2012) was implemented, treating the TFI and CTFI scores as continuous characters. We generated the ACSR using a maximum likelihood approach and the Contmap fuction to map the traits onto the phylogeny.

Variation in TFI as a Function of Diet and Feeding Behavior

After testing for asymmetry, we used Kruskal-Wallis statistical tests and Wilcoxon rank sum tests with Bonferroni adjustments to look for statistical differences in TFI scores related to diet and feeding strategies.

For analyses of diet, we obtained data related to marine odontocete prey from Pauly et al. (1998). Information on the diets of freshwater odontocete species along with sixteen other marine species not listed by Pauly et al. (1998), was collected from Perrin et al. (2009). We classified whales into four different diet categories: fish specialists, squid specialists, generalists that feed on a wide variety of prey, and tetrapod specialists. We classified whale species as fish or squid specialists if the stomach contents consisted of greater than 50% of either prey type. We considered odontocete whale diets in which either prey type did not form the majority of the diet diet (due to consumption of other food items such as benthic invertebrates or higher vertebrates) to be "generalist" feeders. Lastly, whales which were recorded as having other mammals or birds as contributing a significant portion of their diet (40% or more of total prey consumed) were classified as having a diet of tetrapods. *Orcinus* is the only extant species that falls within this latter category.

We divided feeding strategies into four major categories relevant to odontocete whales: ram, snap, suction, and grip-and-tear feeding. Assignment of extant whales to these feeding categories follows Martins et al. (2020), supplemented with data from Galatius et al. (2020) and Coombs et al. (2020). While alternative classifications for feeding behavior exist for marine mammals (e.g., Hocking et al. 2017b), the above categories are all prey capture and processing strategies which we would expect to influence the size of area of attachment for the temporalis muscle, and thus the TFI and CTFI. For taxa in which we found little information on foraging behavior, we inferred feeding strategy using the behavior of congeneric species and overall morphology. Feeding behavior can be flexible, and some taxa use both suction and ram feeding, or there is uncertainty regarding which method may represent the dominant prey capture strategy. This uncertainty has resulted in some of the above references disagreeing on the categorization of certain taxa, namely *Lagenorhynchus acutus* and taxa belonging to the genera *Cephalorhynchus*, *Lagenodelphis*, *Pepenocephala*, *Orcaella*, and the family Phocoenidae. To accommodate these taxa, they were placed in a separate category, ram/suction feeders.

Institutional abbreviations

AMNH = American Museum of Natural History, New York City, New York, USA; **CCNHM**= Mace Brown Museum

of Natural History – College of Charleston, Charleston, South Carolina, USA; **ChM** = The Charleston Museum, Charleston, South Carolina, USA; **DUNUC** = D'Arcy Thompson Zoology Museum, University of Dundee, Dundee, UK; **LACM** = Los Angeles County Natural History Museum, Los Angeles, California, USA; **MNHN** = Museum National d'histoire naturelle, Paris France; **MSNT** = Museo Civico di Storia Naturale di Torino, Torino, Italy; **NHM** = Natural History Museum, London, UK **NMV** = National Museum of Victoria, Melbourne, Australia; **OU** = Otago University, Dunedin, New Zealand; **SDNHM** = San Diego Natural History Museum, San Diego, California, USA; **SMNS** = Staatliches Museum fuer Naturkunde, Stuttgart; Stuttgart, Germany; **UAM** = University of Alaska Museum of the North, Fairbanks, Alaska, USA; **USNM** = National Museum of Natural History, Washington, D.C., USA.

RESULTS

Asymmetry of Temporal Fossa Area

Temporal fossa index values calculated separately for the right and left sides of odontocete whale skulls were significantly different (df = 199; T = -4.60; P = < 0.0001), indicating bilateral asymmetry in the size of the temporal fossa, with the right side slightly larger than the left (Fig. 2). Further paired T-tests performed at the superfamily level determined that significant asymmetry in the size of the temporal fossa was not present in all odontocete clades, but only in certain groups (Table 1). Significant differences in TFI values calculated from each side of the

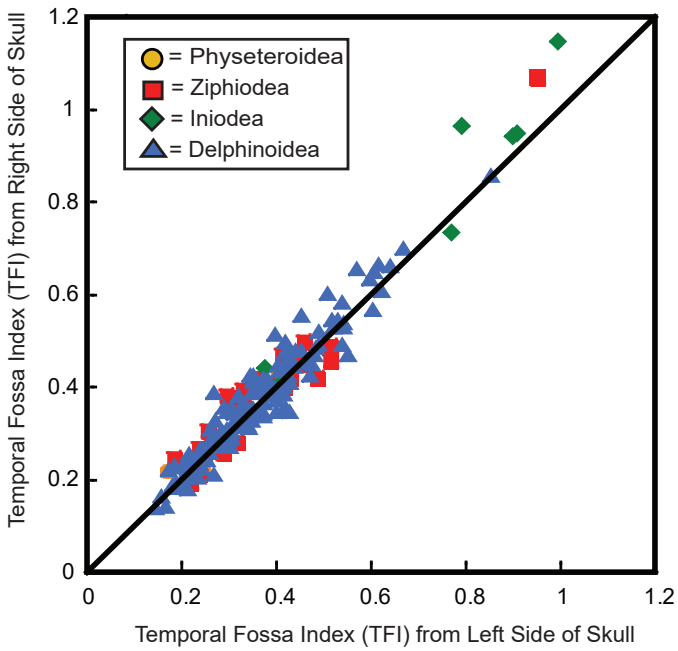

Figure 2. Temporal fossa index (TFI) values calculated from the temporal fossa of the left vs right side of the skull. Taxa on the diagonal line have no or little difference in the TFI values calculated between both sides, while taxa above the line have TFI values that are larger when calculated using the right side, while taxa below the line have TFI values that are larger when calculated using the left side. Symbols represent different major clades of extant odontocete whale. TFI values shown are based on scores from individual specimens (N = 200).

Superfamily	Family: Subfamily	Mean Difference	Degrees of Freedom	t-Value	t-Probability
All Odontocetes	**-**	**-1.22**	**199**	**-4.6**	**< 0.001**
Physeteroidea	-	-1.03	4	-0.86	0.44
Ziphoidea	-	-.77	33	-1.26	0.22
Iniodea	-	-5.68	7	-2.21	0.06
Delphinoidea	**-**	**-1.03**	**151**	**-3.77**	**0.0002**
	Monodontidae	-0.36	3	-0.28	0.80
	Phocoenidae	**-2.33**	**17**	**-3.10**	**0.007**
	Delphinidae: Delphininae	**-0.008**	**78**	**-2.43**	**0.017**
	Delphinidae: Lissodelphininae	-0	23	-0.008	0.99
	Delphinidae: Globicephalinae	**--0.02**	**19**	**-2.68**	**0.015**

Table 1. Paired t-test results for comparison of left versus right temporal fossa area for extant odontocetes. Platanistoidea was excluded from analysis due to a sample size of one. Clades with significant differences in skull asymmetry (represented by a t-probability < 0.05) are in bold.

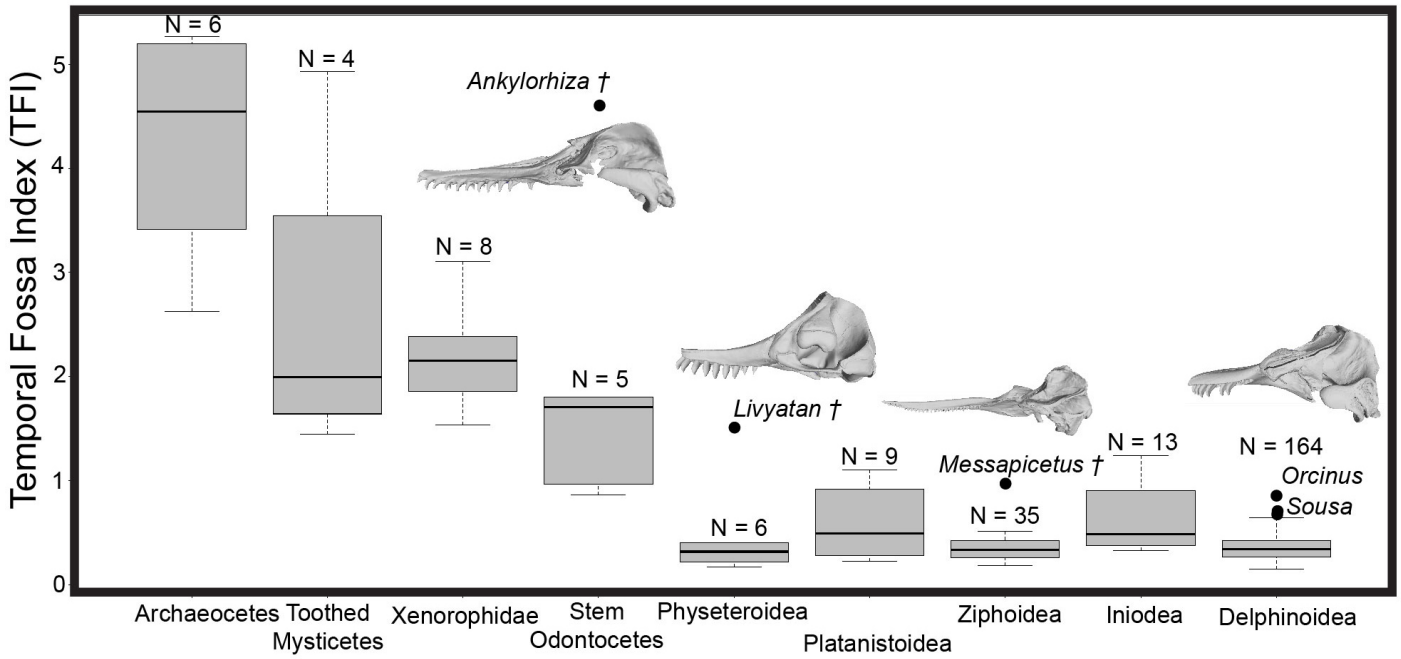

Figure 3. Variation in temporal fossa index (TFI) scores across extant and extinct whales. Outliers are labeled with their genus next to them. Stem odontocetes includes odontocete whales outside the crown group but later diverging than Xenorophidae. Numbers above boxplots represent sample size, and † symbols identify extinct genera. Lateral view images from 3D scans of whales shown for outlier taxa, from left to right *Ankylorhiza tiedemani* (CCNHM 103), *Livyatan melvillei* (MSNUP specimen), *Messapicetus longirostris* (MSNTUP specimen), and *Orcinus orca* (USNM 11980)..

skull are seen in Delphinoidea (mean difference = -1.03; df = 151; T = -3.77; P = 0.0002), but not in Physeteroidea, Ziphioidea, or Inioidea, indicating differences in TFI for the different sides of the skull in odontocetes is being driven entirely by cranial asymmetry in one clade.

We assessed asymmetry within Delphinoidea at the family and subfamily level. Within Delphinoidea, Phocoenidae (mean difference = -2.34; df = 17; T = -3.10; P = 0.007), Delphininae (mean difference = -0.008; df = 78; T = -2.43; P = 0.017) and Globicephalinae (mean difference = -0.02; df = 19; T = -2.67; P = 0.015) exhibited significant differences in TFI between right and left sides (Table 2 and Fig. 2). We did not detect asymmetry within Monodontidae nor Lissodelphinae.

Variation in Temporal Fossa Index (TFI)

Significant differences are evident in the uncorrected TFI scores of extant and extinct whales (df = 8; $\chi 2$ = 74.57; P < 0.001; Table 2 and Fig. 3), especially between various stem whale clades and modern taxa. Overall, archaeocetes had the highest uncorrected TFI scores, while crown odontocetes possessed the lowest scores. Archaeocetes possessed an average TFI score of 4.27, with *Basilosaurus* having the highest TFI score (5.26) and *Zygorhiza* the lowest (2.63); The TFI of *Zygorhiza*, even if it is lower than most other archaeocetes, is still over twice as large as the largest extant odontocete score. We found archaeocete TFI values to be significantly different (Table 3) from those of Xenorophidae (P = 0.05), Platanistoidea (P = 0.01), Ziphioidea (P < 0.001), Inioidea (P = 0.003), and Delphinoidea (P = 0.001). The range of scores seen in archaeocetes overlaps most broadly with those of toothed mysticetes, but they are generally higher than values reported for Xenorophidae or stem odontocetes, with some overlap.

Toothed mysticetes record the next highest TFI scores (mean = 2.59), with *Coronodon* having the largest TFI with a score of 4.93, and *Fucaia* having the lowest, with a score of 1.45. The range of values exhibited by toothed mysticetes is intermediate between those of archaeocete whales and early odontocetes, although showing more similarity and overlap with the former. We recorded significant differences in TFI scores between toothed mysticetes and Ziphioidea (P = 0.009), Inioidea (P = 0.03) and Delphinoidea (P = 0.02).

In contrast to the range of scores possessed by the former two groups of extinct whales, xenorophids exhibit less variation, with a maximum TFI score of 3.1 (*Xenorophus simplicidens*) and a minimum score of 1.53 (*Cotylocara*), with an average TFI of 2.18. Xenorophidae show significant differences from all crown odontocete

Table 2. Probability values produced through Wilcoxon pairwise comparison rank sum tests with Bonferoni adjustment of temporal fossa index (TFI) values from the left side of the skull, by taxonomic group. Stem odontocetes includes odontocete whales outside the crown group but later diverging than Xenorophidae. Values in bold represent significant differences. Numbers in column titles represent sample size of clade.

	Archaeoceti (N = 6)	Toothed Mysticeti (N = 4)	Xenorophidae (N = 8)	Stem Odontoceti (N = 5)	Physeteroidea (N = 6)	Platanistoidea (N = 9)	Ziphiodea (N = 35)	Iniodea (N = 13)	Delphinoidea (N = 164)
Archaeoceti		1.0	**0.05**	0.88	0.08	**0.02**	**< 0.001**	**0.003**	**0.001**
Toothed Mysticeti			1.0	1.0	0.69	0.15	**0.009**	**0.03**	**0.02**
Xenorophidae				1.0	**0.02**	**0.006**	**< 0.001**	**< 0.001**	**< 0.001**
Stem Odontoceti					0.55	0.17	**< 0.001**	**0.05**	**0.001**
Physeteroidea						1.0	1.0	1.0	1.0
Platanistoidea							1.0	1.0	1.0
Ziphiodea								**0.03**	**0.04**
Iniodea									**0.009**

Table 3. Probability values produced through Wilcoxon pairwise comparison rank sum tests with Bonferoni adjustment of temporal fossa index (TFI) values from the left side of the skull, by taxonomic group. Only extant and historically extinct odontocetes included in this table. Values in bold represent significant differences. Numbers in column titles represent sample size of clade. Stem Delphinidae includes *Lagenorhynchus albirostris* and *L. acutus*, two taxa consistently found outside of Lissodelphinae and at the base of Delphinidae. For comparisons within Delphinoidea, see Table 4.

	Physeteridae (N = 1)	Kogiidae (N = 4)	Platanistidae (N = 2)	Ziphiidae (N = 34)	Lipotidae (N = 1)	Pontoporiidae (N = 3)	Iniidae (N = 4)
Physeteridae		1.0	1.0	1.0	1.0	1.0	1.0
Kogiidae			1.0	1.0	1.0	1.0	1.0
Platanistidae				0.28	1.0	1.0	1.0
Ziphiidae					1.0	1.0	**0.003**
Lipotidae						1.0	1.0
Pontoporiidae							1.0
Iniidae							
Monodontidae	1.0	1.0	1.0	**0.009**	1.0	1.0	1.0
Phocoenidae	1.0	1.0	1.0	1.0	1.0	1.0	**0.03**
Stem Delphinidae	1.0	1.0	1.0	1.0	1.0	1.0	1.0
Orcininae	1.0	1.0	1.0	1.0	1.0	1.0	1.0
Lissodelphinae	1.0	1.0	0.48	1.0	1.0	1.0	**0.007**
Globicephalinae	1.0	1.0	0.79	0.42	1.0	1.0	0.31
Delphininae	1.0	1.0	1.0	1.0	1.0	1.0	0.16

groups in TFI score (Table 3). Stem odontocetes, a category which here includes all toothed whales which diverged later than Xenorophidae but before the crown group, also have TFI scores which are elevated compared to crown odontocetes, but have lower scores than archaeocetes, toothed mysticetes, and xenorophids. The exception is the large squalodont-like *Ankylorhiza*, which has an incredibly high TFI score of 4.62, especially when compared to the next highest stem odontocete score, 1.8 for *Eosqualodon*. The TFI score for *Ankylorhiza* is larger than that seen in most toothed mysticetes and xenorophids, and comparable to values recorded for many archaeocete whales. Stem odontocetes are significantly different from Ziphioidea ($P < 0.001$), Inioidea ($P = 0.05$) and Delphinoidea ($P = 0.005$).

Crown odontocetes show a narrower range of variation in TFI when compared to the prior taxonomic categories, with a range from 1.51 to 0.16. Within the crown group, living physeteroids possess low TFI scores (0.17-0.4; mean = 0.29). This is in contrast however to the one extinct physeteroid included, the giant sperm whale *Livyatan*, which had a TFI score of 1.51, larger than any other crown odontocete in this study. We found Physeteroidea to only be significantly different from Xenorophidae of the whales included in this study ($P = 0.02$)

Platanistoidea (range = 0.22-1.11; mean = 0.55) show a diversity in TFI scores, with the modern *Platanista* having a larger TFI (mean = 0.93) than all its extinct relatives. We found no significant difference in TFI score between Platanistoidea and other crown odontocete clades.

Extant members of Ziphioidea exhibit a lower and narrow range of TFI scores (range = 0.18-0.51; mean = 0.34). In contrast, the extinct taxon *Messapicetus* has a TFI score almost twice as large as the largest modern ziphiid score, with a TFI of 0.97. Among crown odontocetes, we only found only Inioidea ($P = 0.03$) to be significantly different from Ziphioidea.

Comparable to the pattern observed in Platanistoidea, we observed a wide variation in TFI scores (range = 0.32 - 0.99; mean = 0.59) when considering modern and extinct inioids together. Besides ziphioids, inioids are also found to be significantly different from delphinoids ($P = 0.009$).

Delphinoids exhibit considerable diversity in TFI scores, with the "kentriodontid" *Atocetus* having the largest TFI score (1.24), followed by the extant *Orcinus* (0.85). The delphinine genus *Sousa* also have unusually large TFI scores, ranging from 0.43 to 0.68. *Monodon* has the smallest TFI score at 0.15. Overall, the mean TFI score for delphinoids is 0.36. Except for *Atocetus*, extinct delphinoids have TFI scores that fit within the range of scores recorded in modern taxa, with *Semirostrum* having the lowest score of any extinct species (0.25), while

Table 4. Probability values produced through Wilcoxon pairwise comparison rank sum tests with Bonferoni adjustment of temporal fossa index (TFI) values from the left side of the skull, by taxonomic group. Results of comparisons of clades within Delphinoidea included in this table. Values in bold represent significant differences. Numbers in column titles represent sample size of clade. Stem Delphinidae includes *Lagenorhynchus albirostris* and *L. acutus*, two taxa consistently found outside of Lissodelphinae and at the base of Delphinidae. For comparisons of delphinoid groups with taxa outside this clade, see Table 3.

	Monodontidae (N = 4)	Phocoenidae (N = 17)	Stem Delphinidae (N = 5)	Orcininae (N = 1)	Lissodelphinae (N = 26)	Globicephalinae (N = 20)	Delphininae (N = 81)
Monodontidae		0.07	1.0	1.0	**0.007**	0.31	0.16
Phocoenidae			1.0	1.0	1.0	0.88	1.0
Stem Delphinidae				1.0	1.0	1.0	1.0
Orcininae					1.0	1.0	1.0
Lissodelphinae						1.0	**0.03**
Globicephalinae							0.13

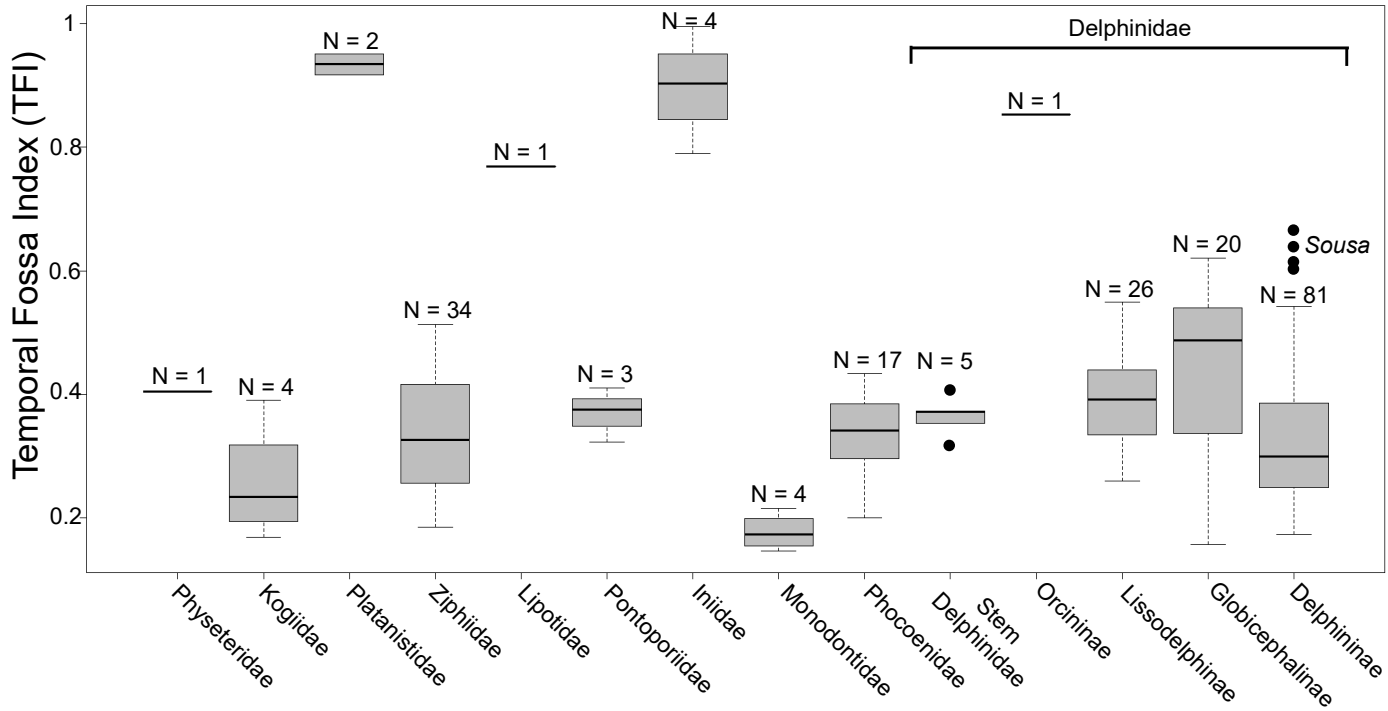

Figure 4. Variation in temporal fossa index (TFI) scores across extant and historically extinct crown group odontocetes. Taxa organized by family, and in the case of Delphinidae, subfamily. Stem Delphinidae includes *Lagenorhynchus albirostris* and *L. acutus*, two taxa consistently found outside of Lissodelphinae and as the earliest diverging members of Delphinidae. Outliers are labeled with their genus name next to them. Numbers above boxplots represent sample size.

other extinct taxa have somewhat higher scores between 0.44 and 0.69.

If we only consider extant odontocetes, an extreme reduction in diversity of TFI scores both for the clade in general as well as for various families that are contained within it is found (Figure 4). When comparing families and subfamilies of extant odontocete whale, significant differences are still found (df = 13; $\chi 2$ = 56.09; P < 0.001; Table 4), although pairwise Wilcoxon rank sum tests find few groups to be significantly different, with only significant differences recovered in Iniidae versus Ziphiidae (P = 0.003), and Lissodelphinae versus Iniidae (P = 0.007), Monodontidae (P = 0.007), and Delphininae (P = 0.03). In part, this is due to reduced taxonomic and ecologic diversity of many living groups, especially the "river dolphin" families. Modern platanistids (mean = 0.93), lipotids (0.76), and iniids (mean = 0.9) all have TFI scores well above the other odontocete clades, only overlapping with *Orcinus*. All other odontocete families and subfamilies have TFI scores generally below 0.6 and exhibit broad overlap, with Monodontidae having the lowest TFI scores (range = 0.15-0.22; mean = 0.18).

When we accounted for variation in telescoping by using the CTFI, much of the variation observed between different extinct whale groups compared to the crown group is removed, although significant differences are still identified (df = 8; $\chi 2$ = 51.77; P < 0.001; Figure 5). Significant differences from pairwise comparisons of CTFI scores are only present between ziphiids and xenorophids (P < 0.001) and stem odontocetes (P < 0.001), as well as between delphinoids and xenorophids (P < 0.001) and stem odontocetes (P = 0.001).

Archaeocetes, rather than having the highest TFI scores, have negative corrected values, including some of the smallest values of any whale in this study. The exception is *Basilosaurus*, whose CTFI score (~1.01) is unusually high. Toothed mysticetes also for the most part have negative corrected values. The one exception is *Coronodon*, which has the second largest recorded CTFI score (1.96) in this study, larger than even *Basilosaurus*.

Xenorophids and stem odontocetes overall show significantly higher CTFI scores than those exhibited by members of the crown group. *Ankylorhiza*, with a CTFI score of 4.18 has the largest value of not only any

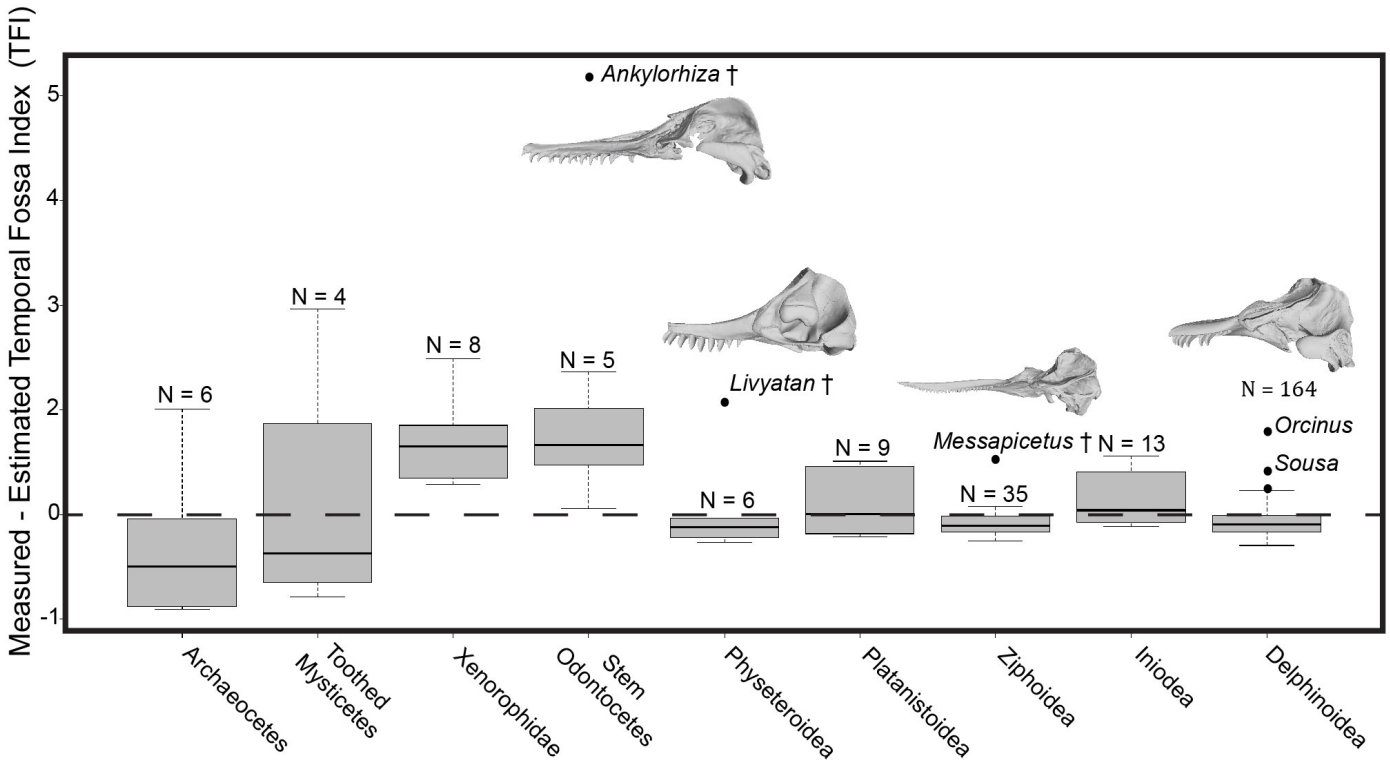

Figure 5. Variation in corrected temporal fossa index (CTFI) scores across extant and extinct whales. Outliers are labeled with their genus next to them. Stem odontocetes includes odontocete whales outside the crown group but later diverging than Xenorophidae. The horizontal dotted line represents where predicted TFI based on length of intertemporal region are equal to estimated values; taxa above this line have larger than expected temporal fossae, while taxa below this line have smaller than expected temporal fossae. Numbers above boxplots represent sample size, and † symbols identify extinct taxa. . Lateral view images from 3D scans of whales shown for outlier taxa, from left to right *Ankylorhiza tiedemani* (CCNHM 103), *Livyatan melvillei* (MSNUP specimen), *Messapicetus longirostris* (MSNTUP specimen), and *Orcinus orca* (USNM 11980).

odontocete in this study, but of any whale, surpassing both *Basilosaurus* and *Coronodon*. *Xenorophus simplicidens* and *Eosqualodon* also have CTFI scores greater than that seen in crown group whales.

Within crown group Odontoceti, most taxa have CTFI scores close to zero, and higher than most archaeocetes but lower than xenorophids and other stem odontocetes. The largest CTFI score we recorded for this clade was possessed by the extinct physeteroid *Livyatan*, which has a CTFI score of ~1.08. Crown physeteroids, ziphiids, and delphinoids show minor degrees of variation in CTFI and have somewhat negative values. Besides *Livyatan*, *Messapicetus*, *Atocetus*, *Orcinus*, and *Sousa* have high CTFI values that are outliers to the normal range of variation for their clades. Platanistoids and inioids show a wider range of variation. *Notocetus* and *Platanista* possess elevated CTFI scores compared to other members of Platanistoidea and *Inia* and *Lipotes* exhibit elevated CTFI scores relative to Inioidea.

Ancestral Character State Reconstruction of Temporal Fossa Index

We detected strong phylogenetic signal in the uncorrected TFI data ($\lambda = 0.997$) and corrected TFI data ($\lambda = 0.991$), indicating that ACSR would be appropriate to apply to this data set. When we mapped TFI data onto our phylogeny (Figure 6), a clear progression of decreasing TFI scores leading to crown Odontoceti is found, with several reversals of this trend in isolated lineages. The earliest diverging whales in this study had extremely high TFI scores (*Ambulocetus* = 4.62; *Aegyptocetus* = 5.19). TFI scores decrease at the base of Pelagiceti and further decrease at the base of Neoceti. However, some species within these clades appear to have reversed these trends, with *Basilosaurus* (TFI = 5.26) and *Coronodon* (TFI = 4.93) having increased TFI scores comparable to that of the earliest archaeocetes.

Most stem odontocetes have TFI scores higher than those possessed by modern taxa, and a significant

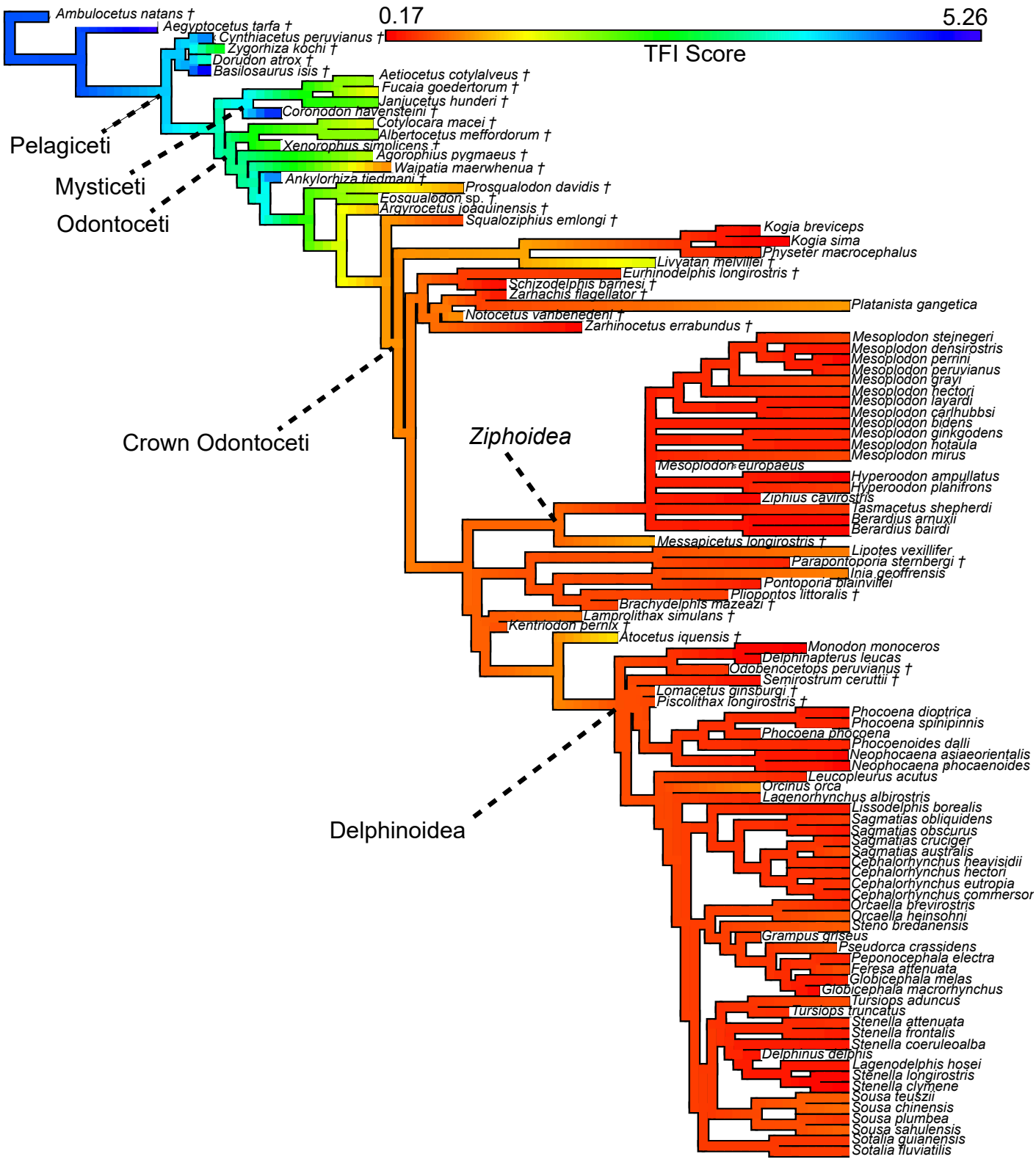

Figure 6. Ancestral character state reconstruction of average temporal fossa index (TFI) scores on a time-calibrated phylogeny of whales. Phylogeny based on Lloyd and Slater (2021) with modifications from McGowen et al. (2020) and Churchill et al. (2018). Significant clades labeled on phylogram. Cool colors represent higher TFI scores, while warm colors represent lower TFI scores.

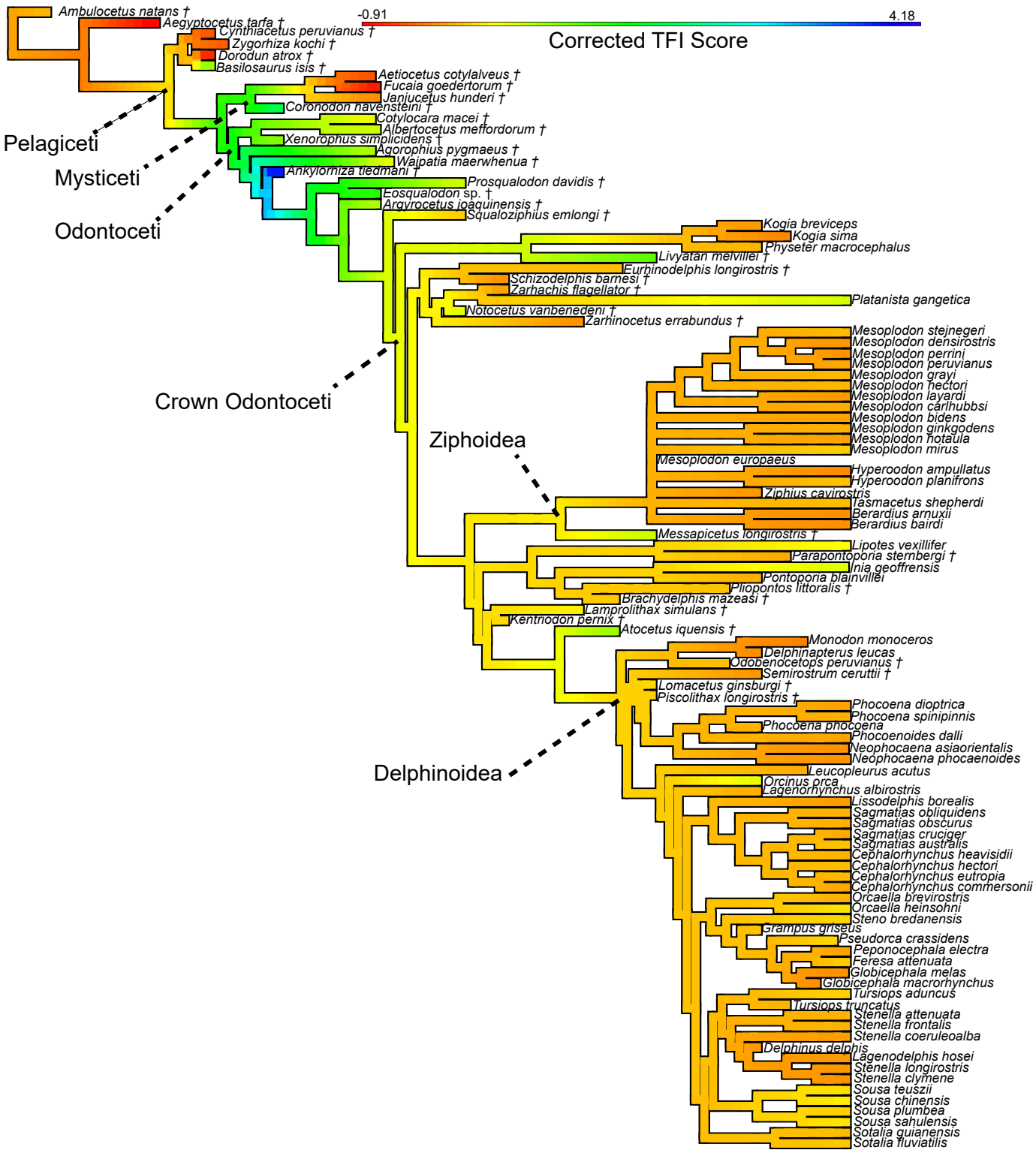

Figure 7. Ancestral character state reconstruction of average corrected temporal fossa index (CTFI) scores on a time-calibrated phylogeny of whales. Phylogeny based on Lloyd and Slater (2021) with modifications from McGowen et al. (2020) and Churchill et al. (2018). Significant clades labeled on phylogram. Cool colors represent higher CTFI scores, while warm colors represent lower CTFI scores.

reduction in TFI appears to evolve at the base of the clade comprising *Argyrocetus* and all later diverging odontocetes, with further reduction at the base of the clade comprising *Squaloziphius* and the crown group. However, several taxa show further independent reductions in TFI scores, including *Waipatia* (TFI = 0.86). At least one stem odontocete shows a reversal towards the ancestral condition, with *Ankylorhiza* having a significantly elevated TFI (TFI = 4.62) compared to the ancestral condition for Odontoceti.

Variation in TFI scores among crown odontocetes is minimal, with little further overall reduction in TFI within the clade. Several lineages however independently increased TFI scores. The most significant of these are *Livyatan* and *Atocetus*, however smaller increases are also evident in *Platanista*, *Messapicetus*, and *Orcinus*.

Removing the influence of telescoping reduced the observed variation in temporal fossa indices and revealed a different pattern of evolution when mapping CTFI scores (Fig. 7). In the CTFI ACSR, archaeocetes were found to have CTFI scores comparable or lower than those of crown odontocetes. The exception to this trend is *Basilosaurus*; even when size and telescoping was accounted for, the resulting CTFI is still far higher than expected (CTFI = 1.01). An increase in CTFI scores is evident at the base of Neoceti, with subsequent independent reversals in Mysticeti and Odontoceti. Reduction in CTFI scores is evident as occurring at the base of the clade including *Janjucetus* and later diverging mysticetes, with further reduction within the aetiocetids.

Within Odontoceti, xenorophids and most stem odontocetes continue to retain CTFI scores higher than extant odontocetes. Amongst these early odontocetes, *Ankylorhiza* is an outlier, with one of the highest CTFI scores of any whale included in this study (CTFI = 4.18). A reduction in CTFI however is evident at the base of the clade containing *Squaloziphius* and crown Odontoceti. Within crown Odontoceti, slight reductions in CTFI scores appear to have independently evolved within crown Physeteroidea, Eurhinodelphinidae, crown Ziphiidae, Inioidea, and Delphinoidea. Reversals to larger CTFI scores within these clades are evident for *Platanista* (CTFI = 0.49), *Lipotes* (CTFI = 0.33), *Inia* (CTFI = 0.46), *Orcinus* (CTFI = 0.41), and *Sousa* (CTFI range of 0.09-0.20).

Temporal Fossa Index (TFI) and Ecology

We found significant differences in TFI scores when diet was examined (DF = 3; $\chi 2$ = 5.07; P = 0.0498; Fig. 8A), although only barely. When pairwise comparisons were made however, no significant differences were found (Table 5), although *Orcinus*, the sole taxa in the analysis to regularly consume higher vertebrates, had a TFI much larger than most other taxa.

We found significant differences in TFI scores (df = 4; $\chi 2$ = 28.96; P < 0.001, Fig. 8B) when comparing taxa based on prey capture behavior. In general, snap feeders and grip-and-tear feeders had the largest recorded TFI values (Fig. 8B), both being statistically different from suction feeders and ram feeders but not from each other (Table 6). Most snap feeding taxa had a TFI score range between 0.76 and 1.0, with a mean of 0.73; the exception was *Pontoporia*, which had low values within the range of ram and suction feeders, with TFI scores between 0.32 and 0.41. *Inia* and *Platanista* had the highest range of values for this prey capture strategy, typically above 0.9. The grip-and-tear feeder *Orcinus* had a TFI of 0.85, while *Pseudorca* had lower TFI values within the range of 0.5-0.6 and a mean of 0.56.

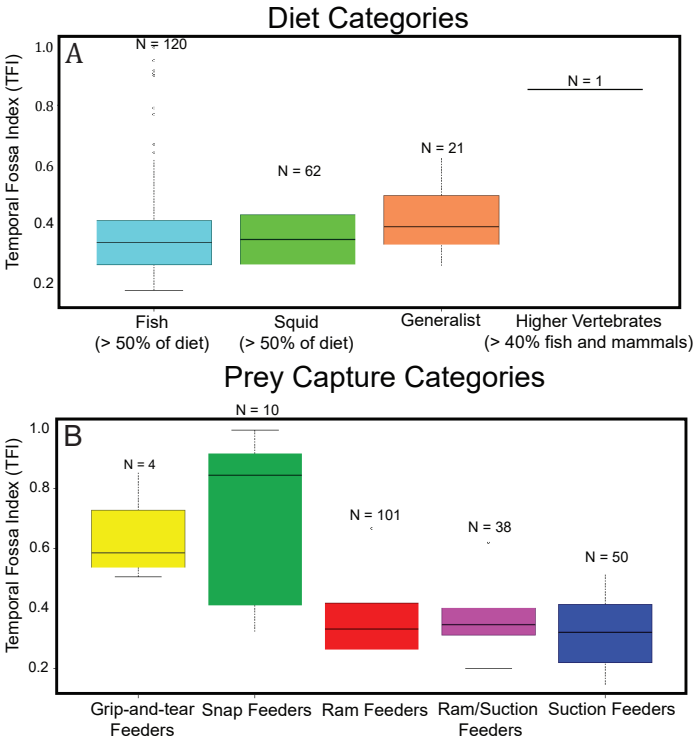

Figure 8A-B. Boxplots showing variation in temporal fossa index (TFI) scores compared to diet (A) and prey capture method (B). Numbers above boxplots represent sample size. Taxa categorized as generalist in A represent species in which neither fish nor squid made up most of the prey consumed, and thus eat a wide variety of prey. Taxa characterized as Ram/Suction feeders in B are taxa that engage in both styles of feeding

Table 5. Probability values produced through Wilcoxon pairwise comparison rank sum tests with Bonferoni adjustment of temporal fossa index (TFI) values from the left side of the skull, by diet. Numbers in column titles represent sample size of clade. No significant differences were found

Diet	Squid (N = 62)	Fish (N = 120)	Generalist (N = 21)	Higher Vertebrates (N = 1)
Squid		1.0	0.34	0.56
Fish			0.14	0.71
Generalist				0.57

Table 6. Probability values produced through Wilcoxon pairwise comparison rank sum tests with Bonferoni adjustment of temporal fossa index (TFI) values from the left side of the skull, by prey capture method. Values in bold represent significant differences. Numbers in column titles represent sample size of clade.

Prey Capture Method	Grip-and-tear (N = 4)	Snap (N = 10)	Ram (N = 101)	Ram and Suction (N = 38)	Suction (N = 50)
Grip-and-tear		1.0	**0.03**	**0.001**	**0.01**
Snap			**< 0.001**	**0.001**	**0.001**
Ram				1.0	1.0
Ram and Suction					1.0
Suction					

The range of values recorded for suction, ram, and taxa which did both were much lower, and almost completely overlapped with one another (Fig. 8B). We detected no statistical difference between these prey capture methods. Ram-feeding taxa had TFI scores ranging from 0.18 to 0.67, with a mean of 0.35, and on the high end overlapping with values reported for *Pseudorca*. Within this range of values, members of the subfamily Delphininae generally had the lowest scores, especially *Delphinus* (mean = 0.27) and *Stenella* (mean = 0.32). Pure suction feeding taxa had TFI scores between 0.15 and 0.51 and a mean of 0.32. Ziphiids had some of the higher TFI scores for a suction feeding whale, while kogiids, monodontids, and *Globicephala* had smallest TFI values. Taxa considered both suction feeders and ram feeders show a range of values from 0.21 to 0.47, and a mean of 0.36.

DISCUSSION

Cranial Telescoping and Temporalis Attachment Area Size

The size of the temporalis muscle, and its variation through time, provides more information than just insights into changes in whale ecology. We can also begin to unravel the complex relationship of mastication, and how the loss of this behavior may have influenced or been influenced by cranial telescoping.

The earliest known whales, the paraphyletic "archaeocetes," possess the proportionally largest temporalis muscles. All archaeocetes whales retained the ability to masticate food from their terrestrial ancestors (Armfield et al. 2013, Fahlke et al. 2013, Thewissen et al. 2011). Their closest known relatives, small raoellids like *Indohyus* (Geisler and Theodor 2009, Thewissen et al. 2007), largely fed on terrestrial vegetation (Thewissen et al. 2011), using water as a refuge to escape from predators, much like modern water chevrotains (Thewissen et al. 2007, Thewissen et al. 2011). Although possessing a diet quite different from the earliest whales, wear patterns indicate a pattern of chewing like that seen in the first whales (Thewissen et al. 2011).

In contrast to the raoellids, the oldest known whales, the pakicetids, were carnivores that actively foraged for food in aquatic environments (Clementz et al. 2006, Roe et al. 1998). Although unrelated to carnivorans, their masticatory apparatus was similar (Fahlke et al. 2013). Pakicetids, as well as the later diverging protocetids, still retained a protocone molar, indicating the ability to grind food (Fahlke et al. 2013, Snively et al. 2015). This ability was lost in later diverging archaeocetes. Analyses of tooth wear in these taxa support a generalized diet of fish and aquatic invertebrates, although some taxa such as *Qaisracetus* and *Babiacetus* may have been more

specialized (Fahlke et al. 2013, Thewissen et al. 2011). It is unlikely that the diet or style of feeding in these taxa would have necessitated greater development of the temporalis muscle, however further study is needed to test this assumption.

The protocone (and grinding function) was lost in later diverging archaeocetes (Fahlke et al. 2013). Mediolaterally compressed postcanines however were likely still used to crush and shear flesh using ortho-retractional occlusal movements (Fahlke et al. 2013). An increase in dental complexity and the evolution of additional tooth cusps and increased sharpness of these cusps suggests a reduced importance for teeth in prey processing overall (Armfield et al. 2013, Thewissen et al. 2011). Rather, the teeth were used more for holding prey than tearing it apart.

While the proportional size of the temporalis muscle in archaeocetes is impressive it is not indicative of any real specialization in diet when contrasted with odontocetes. Rather, archaeocetes show either no or only minor degrees of cranial telescoping (Churchill et al. 2018a, Coombs et al. 2022), and so simply benefit from having more room for a large area of attachment for this muscle. Superficially, TFI values are still greater than those in extant terrestrial artiodactyls, as a casual inspection of several species finds (*Sus domesticus* = 1.67, *Pecari tajacu* = 2.32, *Antilocapra americana* = 0.81, *Odocoileus virginianus* = 1.23), showing an increase in temporalis size at the base of Cetacea. When telescoping is accounted for however, nearly all archaeocetes have temporalis muscles that are modest and unexceptional, with CTFI scores comparable to that found in terrestrial omnivorous artiodactyls like pigs (-0.53) and peccaries (-0.754). The one exception to this trend is *Basilosaurus*. *Basilosaurus* has the largest proportional temporalis muscle of any whale in this study. Even when cranial telescoping is accounted for, this muscle is still inferred to be far larger than that of any modern whale. This finding is consistent with prior studies which have found that *Basilosaurus* was able to exert the largest bite force of any known mammal (Snively et al. 2015). The proportionally large temporalis complements evidence from tooth wear (Fahlke et al. 2013), taphonomy (Fahlke 2012), and stomach contents (Swift and Barnes 1996, Uhen 2004) which indicate a macropredatory lifestyle, placing this whale at the top of the food chain.

Archaeocetes eventually gave rise to the two divergent lineages which comprise living whales, Odontoceti and Mysticeti. The earliest members of both groups were capable of limited mastication, however both clades saw parallel loss of occlusion and tooth complexity concomitant with increases in polydonty and homodonty (Armfield et al. 2013, Peredo et al. 2018a).

Mysticetes show a great deal of variability in the size of the temporalis muscle, although most species have a temporalis that is proportionally smaller than what is seen in archaeocete whales. While this study only included toothed mysticetes, no doubt this variability would have increased had edentulous taxa been included, and future studies should explore the evolution of the temporalis in this suborder of whales. The high degree of variability in size of the temporalis muscle is consistent with prior work that has highlighted the morphological and ecological diversity of early mysticetes (Marx and Fordyce 2015). This diversity includes putative macropredatory hunters (*Janjucetus*; Fitzgerald 2006), benthic and pelagic suction feeders (*Mammalodon (*Fitzgerald 2010) and *Fucaia* (Marx et al. 2015) respectively) and toothed (Aetiocetidae; Deméré et al. 2008) and toothless filter-feeders (Eomysticetidae; Sanders and Barnes 2002). Although our sample size was limited to only four taxa, we were able to capture some of this diversity in our dataset.

Within toothed mysticetes, *Coronodon* had the highest TFI score, and overall was only second to *Basilosaurus* in size of the temporalis muscle. In fact, after correction for telescoping, it is even higher than *Basilosaurus*. The diet and foraging ecology of this taxon have been debated. Aspects of tooth morphology and similarities in wear patterns to archaeocetes point to raptorial feeding (Geisler et al. 2017). However, other characteristics, such as the presence of a wide rostrum, open rostral sutures, and spacing and development of the molars would suggest dental filtration (Boessenecker et al 2023; Geisler et al. 2017). Tooth wear patterns would also suggest that *Coronodon* didn't use its molars to shear flesh, as seen in earlier archaeocetes (Geisler et al. 2017). Other studies have argued against dental filtration, based on the sharpness of the postcanine dentition, isotopes, and differences in wear patterns between *Coronodon* and alleged modern analogs (Hocking et al. 2017a). However, the number of actual modern analogs available for comparison is limited to just two taxa, the highly derived and closely related phocid seals *Hydrurga* and *Lobodon*. Thus, it is unclear whether the characteristics of these seal taxa in relation to dental filtration can be generalized to taxa outside of Carnivora. Raptorial feeding and dental filtration are also not mutually exclusive hypotheses for foraging behavior. For instance, *Hydrurga* is well known for their macropredatory behavior, however the bulk of their

diet consists of krill, especially during winter (Casaux et al. 2009, Hall-Aspland and Rogers 2004, Hocking et al. 2013, Lowry et al. 1988, Øritsland 1977, Siniff and Stone 1985). *Coronodon* may have also had a similar ecology, seasonally shifting diet or opportunistically engaging in macropredation, while filter-feeding on smaller prey items when larger prey was unavailable.

After *Coronodon*, *Janjucetus* had the next highest TFI score within toothed mysticetes. When telescoping was corrected for, the values are comparable to those possessed by *Aetiocetus* and *Fucaia*. This may seem counterintuitive with the original conception of this whale as a macropredator (Fitzgerald 2006). More recently however, *Janjucetus* has been argued to be a suction-feeder, based on its increased rostral width (Fitzgerald 2012). A specialization for suction feeding could well explain the smaller than expected temporalis size when compared to *Coronodon* or archaeocetes.The remaining toothed mysticetes within this study (*Aetiocetus* and *Fucaia*) belong to the Aetiocetidae. Aetiocetids possess TFI scores much lower than either *Coronodon* or *Janjucetus*, although not as low as those seen in crown odontocetes.

In marine mammal paleontology, few topics are debated more than the ecology of aetiocetid whales, given their placement within mysticete phylogeny between earlier toothed taxa and edentulous baleen-bearing taxa. (Berta et al. 2016, Deméré et al. 2008, Ekdale and Deméré 2022, Marx et al. 2016a, Peredo et al. 2018b). There are many hypotheses concerning the evolution of baleen and bulk-feeding that relate to the interpretation of ecology in these whales, but these hypotheses can be sorted into two major models. One model, which can be referred to as the dental filtration model, posits that filter-feeding evolved prior to tooth loss, and suggests that there may have been a transitional phase in mysticete evolution where some taxa retained teeth but also had baleen (Berta et al. 2016, Deméré et al. 2008, Ekdale and Deméré 2022, Geisler et al. 2017). The other model, which we will refer to as the suction-feeding model, posits that mysticetes lost their teeth because of specialization towards suction-feeding, with baleen and filter-feeding evolving later (Fordyce and Marx 2018, Marx et al. 2016a, Peredo et al. 2018b). Our results are ambiguous regarding either hypothesis, other than indicating that *Coronodon* had had a powerful bite, indicating a lack of relative specialization for dental filtration. Aetiocetids would have had a weaker bite, but both taxa within this study do not show the extreme decreases in TFI associated with specialized suction-feeding in odontocetes; decreased TFI and CTFI in these mysticetes could very well relate to continued loss of mastication and decreased utility of dentition in feeding, rather than the evolution of suction-feeding. This is consistent with other parallel trends in stem mysticetes and stem odontocetes, including decreasing tooth size (Boessenecker and Geisler 2023). Additional sampling of other toothed mysticetes along with early edentulous mysticetes may provide further insights into the evolution of feeding within this clade, and the relevance of either model to baleen evolution.

Whether telescoping is corrected for or not, stem odontocetes had larger temporalis muscles than crown odontocetes. These early odontocetes show greater amounts of heterodonty in their dentition and greater tooth and enamel complexity as well as tooth size than modern odontocetes, traits consistent with a continued use of posterior dentition in mastication (Armfield et al. 2013, Boessenecker and Geisler 2023, Ciampaglio et al. 2005, Loch et al. 2015, Peredo et al. 2018a). Our results are consistent with this interpretation, as based on relative size of the temporalis muscle these whales would have had a stronger bite than living odontocetes. The only exception to this trend is *Squaloziphius*, a taxon often placed just outside the crown group (Geisler et al. 2014, Geisler and Sanders 2003, Lambert et al. 2018, Vélez-Juarbe 2017). It has much lower TFI scores than other stem odontocetes and suggests that the loss of mastication precedes the evolution of the crown group. Later odontocetes would continue to simplify dentition, with different lineages becoming specialized for suction feeding (Boessenecker et al. 2017), and some species becoming completely edentulous (Davit-Béal et al. 2009). As odontocetes lost the ability to masticate entirely, the proportional size of the temporalis muscle also shrank.

Traditionally, studies on whale evolution have treated the simplification of dentition and change in cranial telescoping as two unrelated processes, however our study suggests that the two processes might be closely linked. Cranial telescoping describes the process where the skull is shortened and overlapping of bones occurs (Churchill et al. 2018a, Miller 1923, Roston and Roth 2019). Two different modes of telescoping are recognized (Churchill et al. 2018a): prograde telescoping which is dominant in mysticetes and involves the anterior displacement of the supraoccipital; and retrograde telescoping, dominant in odontocetes, which involves the posterior displacement of facial bones onto the vertex of the skull. Regardless of the mode of telescoping, both processes result in the shrinking and eventual elimination of the intertemporal region dorsally, reducing the available area of attachment for the temporalis muscle (Churchill et al. 2018a, Galatius et al. 2020).

This process of telescoping evolved rapidly, with the earliest known odontocetes already exhibiting some degree of telescoping, and telescoping comparable to what is seen in modern whales was already present before the close of the Oligocene (Churchill et al. 2018a). This creates an interesting question: did reduced importance of the temporalis muscle for feeding enable the further advancement of cranial telescoping, or did the evolution of telescoping induce changes in prey processing? By comparing the TFI and CTFI scores, we can observe a distinct pattern of compensation. That is, as telescoping increased, the proportional size of the temporalis muscle seems to have also increased to compensate for a reduced area of attachment. While an ecological signal is present in the CTFI scores, the variation observed may be better explained by changes in mastication. This would explain why taxa with lesser degrees of telescoping, such as xenorophids and other stem-odontocetes, have higher TFI scores. In crown odontocetes, CTFI scores are generally lower than those of stem whales. This suggests that the area of attachment for the temporalis could proportionally decrease further once mastication was completely lost.

Changes in prey processing ability and dentition clearly predate cranial telescoping. Parallel trends in tooth simplification and reduced dental complexity are present in other marine tetrapod groups (Churchill and Clementz 2016, Ciampaglio et al. 2005). Suction feeding for instance also evolved in pinnipeds and is correlated with dental changes like those present in whales (Adam and Berta 2002, Boessenecker and Churchill 2021). However, retrograde telescoping of the magnitude seen in odontocetes is unique and is linked to the evolution of echolocation (Oelschläger 1990, Rauschmann et al. 2006). Echolocation evolved early in odontocetes and is present in taxa which already show a high degree of telescoping (Churchill et al. 2016, Geisler et al. 2014, Park et al. 2016). We would posit that while retrograde cranial telescoping was likely driven by adaptations for echolocation, that those changes were only possible due to the reduction and decreased importance of mastication in feeding within these whales. A comparable relationship has also been recently suggested for another important masticatory muscle, the masseter, which is homologous to the extramandibular fat body of odontocetes and is responsible for conduction of sound to the ear, important for echolocation (Cozzi et al. 2017, Takeuchi et al. 2024). As the extramandibular fat body developed, the masseter was significantly reduced (Takeuchi et al. 2024). Had mastication still been important in feeding, it is likely that cranial telescoping as seen in odontocetes would have been more minor or taken a much different form.

Temporalis Size and Paleoecological Inference

When examining the relationship between a TFI scores and ecology, there is little direct correlation between diet and TFI, however there is a clear relationship between TFI and prey capture and processing technique. All modern whales can mostly be placed into two convenient groups: a "non-biting" group, consisting of ram and suction feeding whales which have relatively low TFI scores, and a "biting" group, consisting of snap and grip-and-tear feeding whales, which have relatively high TFI scores. Within the biting group, it's not possible to distinguish by TFI scores between these two categories of prey capture and processing. However, within the non-biting group, suction feeding specialists often have somewhat lower TFI values than ram-feeders, although this tendency lacks statistical significance.

The non-biting and biting morphospaces show some overlap (Fig. 9), although the degree of overlap is significantly influenced by the categorization of *Pontoporia*. The Fransiscana (*Pontoporia blainvillei*) is the sole living representative of Pontoporiidae and represents one of the few surviving members of the formerly more diverse inioid radiation of dolphins. Like other inioid dolphins, this species has long rostrum and has been traditionally considered a snap-feeding whale (Berta and Lanzetti 2020, McCurry et al. 2017a, McCurry et al. 2017b). However, the average TFI score is much lower than that of other extant snap-feeding whales (TFI = 0.40, in contrast to 1.07 for *Platanista*, 0.73 for *Lipotes*, and 1.00 for *Inia*). *Pontoporia* also differs from other extant snap-feeding whales in its smaller body size, somewhat more delicate rostrum, and marine habits. The actual foraging behavior of this taxon remains poorly known, although available evidence indicates that it often feeds benthically and has an otherwise generalist diet (Botta et al. 2022). Observational data on prey capture remains lacking for this species, with most inferences on feeding ecology coming from stomach content analysis (Botta et al. 2022, Campos et al. 2020, Fitch and Brownell 1971, Henning et al. 2017, Rodríguez et al. 2002, Tellechea et al. 2017) and isotopes (Di Beneditto and Monteiro 2015, Troina et al. 2016, Viola et al. 2017). Assumptions that this taxon feeds in a manner like *Inia* or *Platanista* may be incorrect. If *Pontoporia* is correctly inferred to be a snap-feeding whale, then there is significant overlap between the biting and non-biting morphospaces, making inferences of feeding behavior more uncertain. If *Pontoporia* is not a snap-feeding taxon, then the area of

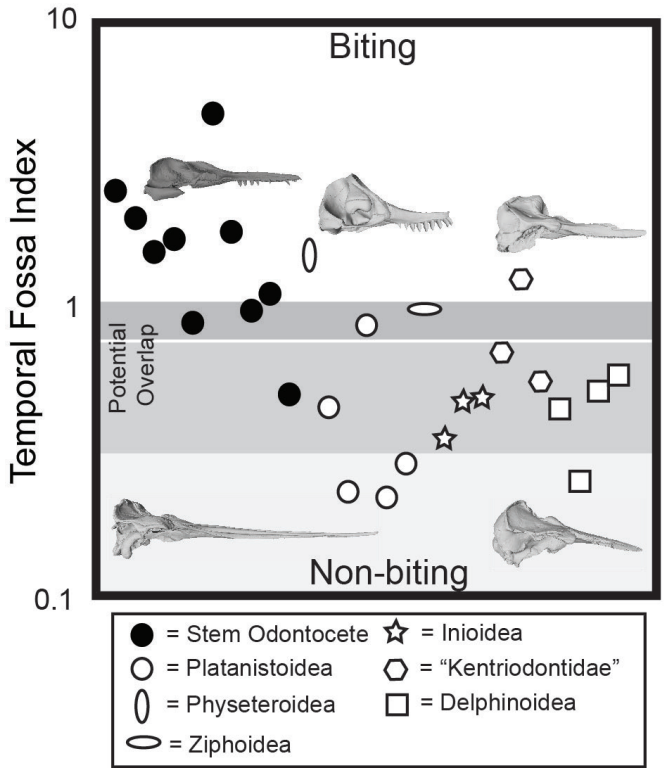

Figure 9. Inference of prey capture and processing behavior in extinct odontocete whales, using the temporal fossa index (TFI). Taxa towards the top of the plot rely upon using a powerful bit during prey capture and processing, including snap and macropredatory grip-and-tear feeders. Taxa towards the bottom of the plot are less likely to use biting, including taxa which club prey with their elongated rostra or suction feed. Darker gray areas in the center represent region of overlap, based on whether *Pontoporia* is considered a snap-feeding whale (lower less dark gray bar) or not (upper dark gray bar). . Lateral view images from 3D scans of from representative taxa found in each section of the morphospace. In the biting section of the morphospace, left to right, *Agorophius pygmaeus* (CCNHM 624), *Livyatan melvillei* (MSNUP specimen), and *Atocetus iquensis* (MNHN.F.PPI 115). In the nonbiting morphospace, from left to right, *Xiphiacetus cristatus* (USNM 21363) and *Semirostrum cerutti* (SDSNH 65276).

overlap is minor, and most extinct whales can be easily placed in either the biting or nonbiting morphospaces.

To infer the ecology of extinct odontocetes, we plotted their TFI scores against the TFI score range for extant biting and non-biting whales (Fig. 9), with the area of overlap illustrated based on both *Pontoporia* being a biting or a non-biting predator. As mentioned in the prior section, almost all stem odontocetes clearly plot within the biting morphospace. The only exception was *Squaloziphius*, which had the lowest score of any stem odontocete and plotted either in the non-biting region or in region overlap between biting and non-biting. Squaloziphiids, although having some similarities to ziphiids, are not considered suction feeders (Lambert et al. 2019), and the TFI scores are high enough to support this supposition.

While *Squaloziphius* had an unusually low TFI score for a stem odontocete, *Ankylorhiza* had an unusually large one, with the largest TFI score of any odontocete. This difference is magnified even more when telescoping is accounted for. This finding is consistent with previous work documenting this taxon as having the largest proportional temporal fossae of any odontocete whale (Boessenecker et al. 2020). The unusually high TFI score, alongside the large body size, severe tooth breakage, and overall cranial and dental morphology (Boessenecker et al. 2020), support the previous hypothesis that *Ankylorhiza* was a macropredatory dolphin, and a major predator on other whales and similar large-bodied prey.

The crown odontocete with the highest TFI score (living or extinct), clearly placing it within the biting morphospace, is the basal physeteroid *Livyatan*. *Livyatan* has been previously suggested to have macropredatory habits, based on a possession of a proportionally large orbit, large body size, robust teeth, and short and broad rostrum (Churchill and Baltz 2021, Lambert et al. 2014, Lambert et al. 2010). We predicted a high TFI score for this taxon which we recovered, as the enormous size of the temporal fossa has been previously commented on (Lambert et al. 2010).

Within our study, platanistoids show a wide variability in TFI scores. Although the modern *Platanista* is a specialized snap-feeder, only one extinct platanistoid has a TFI score indicative of this, *Notocetus* (TFI = 0.88). In fact, *Zarhachis*, *Zarhinocetus*, and *Schizodelphis* have some of the lowest TFI scores of any whale, clearly placing them in the non-biting morphospace. These species, along with *Eurhinodelphis,* possess a proportionally lengthened rostra taken to an extreme not seen in modern odontocetes, and are categorized as "hyper-longirostrine" taxa. Rather than snatching prey between their jaws as snap-feeding taxa do, these species would have first clubbed and stunned prey using rapid lateral or lateral and dorsal movements of the rostra, in a manner like that practiced by modern swordfish and billfish, as suggested byMcCurry and Pyenson (2019). This style of prey capture doesn't require a strong bite, and hence the temporal

fossa area is extremely reduced; hyper-longirostrine taxa have amongst the smallest TFI scores recorded of any whale in this study. *Parapontoporia*, an inioid whale, also had a proportionally long rostrum and low TFI scores, suggesting a similar method of feeding. Our study suggests that snap-feeding and rostral stunning feeding styles, although both involving lengthy rostra, can be readily distinguished by TFI score alone. This may prove useful for inferring the ecology of taxa with more incomplete cranial material; the braincase is often only portion of the skull preserved for many extinct taxa, with the long and fragile rostra either missing or incomplete. TFI scores can thus be used to infer the feeding behavior of extinct odontocetes when rostral length is unknown.

Extinct ziphiids are represented in this study by a single taxon, the Late Miocene *Messapicetus*. *Messapicetus* has a significantly higher TFI score than any living ziphiid. All extant ziphiids are generally considered to suction-feeders (Heyning and Mead 1996). Nearly all living species are edentulous, the one exception being the Southern Hemisphere *Tasmacetus*, which still retains a full complement of teeth in both the upper and lower jaw. Despite the retention of teeth, *Tasmacetus* has a TFI score (0.46), within the range of values possessed by edentulous taxa, although on the higher end of that range. This is much lower than the TFI score of *Messapicetus* with a high score of 0.97. This high score when combined with the elongated rostrum of this taxon (Bianucci et al. 2010) suggest a snap-feeding specialization, or at the very least a mode of feeding different from modern ziphiids.

Three extinct inioids are included in this study; the aforementioned lipotid *Parapontoporia*, and the pontoporiids *Pliopontos* and *Brachydelphis*. While *Parapontoporia* had relatively low TFI scores suggesting similarities in ecology to rostral stunning platanistoids, *Pliopontos and Brachydelphis* have moderate TFI scores similar to that of the extant *Pontoporia*, and likely were similar in ecology. *Brachydelphis mazeasi*, the species included in this study, has frequently been argued to be specialized for suction feeding due to its proportionally short rostra (Lambert and De Muizon 2013). However, our study finds that the TFI score is not particularly low, and within the range of both ram and suction feeding taxa. This suggests that this taxon isn't as specialized for this mode of feeding as some studies would indicate or suggests that the size of the temporal fossa may evolve slower than rostral length proportions.

Three taxa often considered to belong to the paraphyletic Kentriodontidae are included in this study: *Atocetus*, *Lamprolithax*, and *Kentriodon*. After *Livyatan*, *Atocetus* had the next highest TFI score of any extinct crown odontocete. The exact phylogenetic affinities of this taxa have been debated: It's been considered part of a paraphyletic Kentriodontidae, and phylogenetic analysis have placed it either as just outside of Delphinoidea (Barnes 1985, Guo and Kohno 2021, 2023, Lloyd and Slater 2021, Muizon 1988a, Muizon 1988b), just outside both Inioidea and Delphinoidea (Kimura and Hasegawa 2019, Lambert et al. 2017, Peredo et al. 2018c), or within Pontoporiidae (Post et al. 2017). *Atocetus* had a long and robust rostrum which suggests it was a generalized snap-feeding predator, relying on a powerful bite when feeding, as previously suggested for this taxon (Barnes 1985). However, the TFI scores are much higher than those seen by any snap-feeding taxa in our study, and also higher than the presumed ancestral condition. The only crown whale with a higher score is in fact *Livyatan*. At only around two meters in body length (Barnes 1985), *Atocetus* was unlikely to have been a macropredator, but may have targeted larger prey than is typical for a dolphin of this size. *Lamprolithax* and *Kentriodon* in contrast had lower TFI scores that are within the range exhibited by modern delphinoids. Most likely they practiced some combination of ram and/or suction-feeding.

Finally, four extinct taxa assigned to the clade Delphinoidea were included in this study: the bizarre walrus whale *Odobenocetops* and three phocoenids, including the equally odd *Semirostrum* and the more "typical" *Lomacetus* and *Piscolithax*. *Odobenocetops* has often been considered a specialized suction feeder, due to its convergence in morphology (including lack of teeth other than tusks, blunt rostrum, and wide and deeply concave palate) with the walrus *Odobenus* (Muizon 1993, Muizon and Domning 2002). Despite this assertion, the TFI score isn't particularly low, and is comparable to that seen in more typical ram and suction feeders. However, the skull of this taxa is so heavily modified when compared to other crown odontocetes direct comparisons with more typical whales may be misleading.

One of the lowest TFI scores possessed by any taxa, comparable to that exhibited by hyper-longirostrine feeders and well withing the non-biting morphospace, was possessed by the "skimmer porpoise" *Semirostrum*. Unlike all other porpoises, *Semirostrum* possesses an extremely elongated mandible, that extends well past the terminus of the rostrum. Morphology of the mandible along with dental wear has suggested that this species was specialized for benthic feeding, probing the muddy sea bottom with the mandible and using suction to inhale any disturbed prey (Racicot et al. 2014, Racicot

and Rowe 2014). The TFI score recorded for this taxon clearly indicates a diminished use of the temporalis muscle, consistent with this hypothesis. *Lamprolithax* and *Piscolithax* in contrast possess TFI scores comparable to or only slightly higher than that exhibited by modern porpoises, and probably practiced a combination of suction and ram-feeding.

When data from extinct taxa and extant taxa are considered together, we can easily infer two main trends in the data revealed from the TFI scores. The first concerns the loss of mastication, resulting in a concomitant decrease in TFI scores, which preceded the evolution of the crown group. After mastication was lost, TFI scores remained comparatively low, although stem taxa often had larger TFI scores than extant taxa such as delphinids. However, we can see multiple instances where different lineages show increases in TFI scores, associated with specialization towards macropredation (*Livyatan, Orcinus, Atocetus*?) or snap-feeding (*Platanista, Lipotes, Inia, Sousa*?). We also see decreases in TFI scores, which seem to be associated with hyper-longirostrine taxa (Eurhinodelphidae, *Parapontoporia*) or suction feeding (Monodontidae, *Semirostrum*), although these decreases are less dramatic. The same pattern parallels the multiple times rostral length increased and decreased through whale phylogeny, in association with hyper-longirostrine modes of feeding or suction feeding (Boessenecker et al. 2017). This highlights the plasticity in the whale feeding apparatus, and how unrelated odontocetes can converge on the same morphologies when similar modes of feeding evolve.

Asymmetry in Temporalis Attachment Area

Cranial asymmetry has been observed in all ten extant Odontocete families (Ness 1967). In whale cranial asymmetry, facial bones and features such as the bony nares, premaxilla and maxilla are shifted to the left making the right side of the face appear larger (Coombs et al. 2020, Huggenberger et al. 2017, Ness 1967). Cranial asymmetry in whales has been suggested to be related to prey size (Macleod et al. 2007), but more commonly has been linked to the evolution of biosonar (Coombs et al. 2020, Heyning 1989, Heyning and Mead 1990, Huggenberger et al. 2017, Mead 1975).

We expected to see no significant differences in size between the left and right temporal fossa area in odontocetes. Cranial asymmetry is well-documented for whales in the facial region (Coombs et al. 2020), but not within the temporal fossa. Additionally, qualitative examination of the skull does not reveal any obvious qualitative differences in anatomy for these regions between the left and right side. There are two potential hypotheses that may explain the discovery of asymmetry in the size of the area of attachment for the temporalis muscle. First, cranial asymmetry in the facial region that is found in odontocete whales may have impacted the way the temporal fossa developed. Genes controlling the development of asymmetry in the facial region may in turn influence the development of the rest of the skull, thus inducing asymmetry in the temporal fossa, despite the lack of any adaptive significance of this region for echolocation. Cranial asymmetry may also explain why the right temporal fossa appeared larger than the left in this study; the facial midline in odontocetes is skewed left making the right side of the face larger (Churchill et al. 2018b, Coombs et al. 2020). However, degrees of asymmetry in the facial region don't align with the patterns of asymmetry we noticed for the temporal region. Phocoenid skulls appear more symmetrical than skulls from the physeteroid *Kogia,* with *Kogia* having one of the most asymmetrical skulls of any whale (Coombs et al. 2020, Huggenberger et al. 2017). However, we found no evidence of temporal fossa asymmetry in *Kogia*, while it was detected in phocoenids, the opposite of the pattern we would expect if this hypothesis was true. It appears then that facial asymmetry has no association or influence on temporal fossa asymmetry.

A second hypothesis that could possibly explain the skull asymmetry found in temporal fossa area in this study is lateralization. Lateralization occurs when an animal prefers to use one side of their body or body part over the other despite being able to use both (Mutha et al. 2012). A preference for rightward feeding tendencies is well documented in whales, resulting in whales preferentially lunging to the right during prey capture movements (MacNeilage 2013). This preference can result in increased wear and abrasion to baleen plates and mandibles (Canning et al. 2011, Clapham et al. 1995, Kasuya and Rice 1970), or laterally biased injuries during feeding (Beatty and Dooley 2009). While best studied in baleen whales, right-side bias in foraging behaviors has also been documented on multiple occasions in *Tursiops* (Kaplan et al. 2019, Karenina et al. 2016) as well as in *Neophocaena* (Amano et al. 2021), resulting in increased abrasions to the right teeth and side of the mandible (Karenina et al. 2016). The possibility of lateralization playing a role in explaining the observed asymmetry is intriguing, but further evidence from quantitative studies of odontocete behavior and jaw movements are needed to evaluate this hypothesis.

CONCLUSIONS

The area of attachment for the temporalis muscle varies significantly in size within whales. Archaeocetes have proportionally enormous areas of attachment, but as mastication is lost the size of this muscle attachment decreases, with toothed mysticetes and stem odontocetes having smaller proportional areas, and crown odontocetes having even smaller areas of attachment. This reduction in the importance of mastication and subsequent decrease in size of the temporalis may have enabled increased telescoping of the skull as exhibited in living whales. Beyond this overall trend, method of prey capture significantly influence the size of the proportional area of attachment. Snap-feeders and macropredatory grip-and-tear feeders possess enormous temporalis muscles providing a powerful bite. The area of attachment for the temporalis muscle in these taxa are much larger than the area of attachment possessed by suction and ram-feeding whales, which have little use for a powerful bite. This pattern can be used to infer the feeding behavior of extinct taxa. *Basilosaurus*, *Coronodon*, *Ankylorhiza*, and *Livyatan* all possess large temporalis muscles consistent with macropredatory behavior, while *Notocetus* was likely a snap-feeder. Taxa with proportionally small areas of attachment include hyper-longirostrine taxa such as eurhinodelphids, *Zarhachis*, and *Parapontoporia*, who likely relied upon rostral stunning and didn't require a strong bite for prey capture. *Semirostrum*, a proposed benthic skimming porpoise, also possessed an unusually small temporalis. Overall, the specific indices developed by this study, the TFI and the CTFI, provide a useful tool for the delimitation of feeding function in extinct whale taxa. Further work should refine these measures and examine other proxies for the size of the temporalis muscle, such as potential width of the temporalis muscle, as well as combine these metrics with other morphological features such as dental form and rostrum length to better quantify the ecology and structure of extinct whale communities

ACKNOWLEDGMENTS

For access to specimens, we thank M. McGowen, J. Ososky, D. Bohaska, N. Pyenson (USNM); S. and R. Boessenecker (CCNHM); M. Gibson and J. Peragine (ChM); N. Simmons, E. Westwig, and E. Hoeger (AMNH), and T. Deméré, K. Randall, and P. Unitt (SDNHM). For access to additional scan data, we would like to thank E. Coombs (UCL), G. Billet (MNHN) and R. Bennion (UL). For assistance with scanning we would also like to thank J. Miguel (NYIT) and B. Young (UWO). For help with collection of measurement data, we also thank C. Baltz and G. Matt (UWO). Funding was provided by the UWO McNair Scholars Program.

LITERATURE CITED

Adam, P. J., and A. Berta. 2002. Evolution of prey capture strategies and diet in the Pinnipedimorpha (Mammalia, Carnivora). *Oryctos* 4:83-107.

Amano, M., Y. Kawano, T. Kubo, T. Kuwahara, and H. Kobayashi. 2021. Population-level laterality in foraging finless porpoises. *Scientific Reports* 11:1-7.

Armfield, B. A., Z. Zheng, S. Bajpai, C. J. Vinyard, and J. G. M. Thewissen. 2013. Development and evolution of the unique cetacean dentition. *PeerJ* 1:e24.

Bapst, D. W. 2012. Paleotree: an R package for paleontological and phylogenetic analyses of evolution. *Methods in Ecology and Evolution* 3:803-807.

Barnes, L. G. 1985. The Late Miocene dolphin *Pithanodelphis* Abel, 1905 (Cetacea: Kentriodontidae) from California. *Contributions in Science, Natural History Museum of Los Angeles County* 367:1-27.

Beatty, B. L., and A. C. Dooley. 2009. Injuries in a mysticete skeleton from the Miocene of Virginia, with a discussion of buoyancy and the primitive feeding mode in the Chaeomysticeti. *Jeffersoniana* 20:1-28.

Berta, A., and A. Lanzetti. 2020. Feeding in marine mammals: an integration of evolution and ecology through time. *Palaeontologia Electronica* 23:a40.

Berta, A., A. Lanzetti, E. G. Ekdale, and T. A. Deméré. 2016. From teeth to baleen and raptorial to bulk filter feeding in mysticete cetaceans: the role of paleontological, genetic, and geochemical data in feeding evolution and ecology. *Integrative and Comparative Biology* 56:1271-1284.

Bianucci, G., O. Lambert, and K. Post. 2010. High concentration of long-snouted beaked whales (Genus *Messapicetus*) from the Miocene of Peru. *Palaeontology* 53:1077-1098.

Bloodworth, B., and C. D. Marshall. 2005. Feeding kinematics of *Kogia* and *Tursiops* (Odontoceti: Cetacea): characterization of suction and ram feeding. *Journal of Experimental Biology* 208:3721-3730.

Boessenecker, R.W., B.L. Beatty, J.H. Geisler. 2023. New specimens and species of the Oligocene toothed baleen whale *Coronodon* from South Carolina and the origin of Neoceti. *PeerJ* 11:e14795

Boessenecker, R. W., and M. Churchill. 2021. The surprising evolutionary heritage of the Atlantic walrus as chronicled by the fossil record. Pp. 9-37. *In* X. Keighley, M. Tange Olsen, P. Jordan, and S. Desjardins, eds. The Atlantic Walrus: Multidisciplinary Insights into Human-animal Interactions. Academic Press London.

Boessenecker, R. W., M. Churchill, E. A. Buchholtz, B. L. Beatty, and J. H. Geisler. 2020. Convergent evolution of swimming adaptations in modern whales revealed by a large macrophagous dolphin from the Oligocene of South Carolina.

Current Biology 30:1-7.

Boessenecker, R. W., D. Fraser, M. Churchill, and J. H. Geisler. 2017. A toothless dwarf dolphin (Odontoceti: Xenorophidae) points to explosive feeding diversifaction of modern whales (Neoceti). *Proceedings of the Royal Society B*. 284:20170531.

Boessenecker, R.W., and J.H. Geisler. 2023. New skeletons of the ancient dolphin *Xenorophus sloanii* and *Xenorophus simplicidens* sp. nov. (Mammalia, Cetacea) from the Oligocene of South Carolina and the ontogeny, functional anatomy, asymmetry, pathology, and evolution of the earliest odontocete. *Diversity*. 1154

Botta, S., M. Bassoi, and G. C. Troina. 2022. Overview of franciscana diet. Pp. 15-48. *In* P. C. Simoes-Lopes, and M. J. Cremer, eds. The Franciscana Dolphin: On the Edge of Survival. Academic Press, London.

Campos, L. B., X. M. Lopes, E. da Silva, and M. C. de Oliveira Santos. 2020. Feeding habits of the franciscana dolphin (*Pontoporia blainvillei*) in south-eastern Brazil. *Journal of the Marine Biological Association of the United Kingdom* 100:300-313.

Canning, C., D. Crain, T. Scott Eaton, K. Nuessly, A. Friedlander, T. Hurst, S. Parks, C. Ware, D. Wiley, and M. Weinrich. 2011. Population-level lateralized feeding behavior in North Atlantic humpback whales, *Megaptera novaeangliae*. *Animal Behavior* 82:901-909.

Casaux, R., A. Baroni, A. Ramón, A. Carlini, M. Bertolin, and C. Y. DiPrinzio. 2009. Diet of the leopard seal *Hydrurga leptonyx* at the Danco Coast, Antarctic Peninsula. *Polar Biology* 32:307-310.

Churchill, M., and C. Baltz. 2021. Evolution of orbit size in toothed whales. *Journal of Anatomy* 239:1419-1437.

Churchill, M., and M. T. Clementz. 2016. The evolution of aquatic feeding in seals: Insights from *Enaliarctos* (Carnivora: Pinnipedimorpha), the oldest known seal. *Journal of Evolutionary Biology* 29(3):19-34.

Churchill, M., J. H. Geisler, B. L. Beatty, and A. Goswami. 2018a. Evolution of cranial telescoping in echolocating whales. *Evolution* 72(5):1092-1108.

Churchill, M., M. R. Martinez, C. Muizon, J. H. Geisler, and J. Mnieckowski. 2016. The origin of high frequency hearing in whales. *Current Biology* 16(16):2144-2149.

Churchill, M., J. Miguel, B. L. Beatty, A. Goswami, and J. H. Geisler. 2018b. Asymmetry drives modularity of the skull in the common dolphin. *Biological Journal of the Linnean Society* 126:225-239.

Ciampaglio, C. N., G. A. Wray, and B. H. Corliss. 2005. A tooth tale of evolution: convergence in tooth morphology among marine Mesozoic - Cenozoic sharks, reptiles, and mammals. *The Sedimentary Record* 3:4-8.

Clapham, P. J., E. Leimkuhler, B. K. Gray, and D. K. Mattila. 1995. Do humpback whales exhibit lateralized behavior. *Animal Behavior* 50:73-82.

Clementz, M. T., A. Goswami, P. D. Gingerich, and P. L. Koch. 2006. Isotopic records from early whales and sea cows: contrasting patterns of ecological transition. *Journal of Vertebrate Paleontology* 26(2):355-370.

Coombs, E. J., J. Clavel, T. Park, M. Churchill, and A. Goswami. 2020. Wonkey whales: the evolution of cranial asymmetry in cetaceans. *BMC Biology* 18(86):1-24.

Coombs, E. J., R. N. Felice, J. Clavel, T. Park, R. F. Bennion, Author, J. H. Geisler, B. L. Beatty, and A. Goswami. 2022. The tempo of cetacean cranial evolution. *Current Biology* 32(10):2233-2247.

Cozzi, B., S. Huggenberger, and H. A. Oelschläger. 2017. Anatomy of Dolphins: Insights into Body Structure and Function. Elsevier, London, UK.

Davit-Béal, T., A. S. Tucker, and J. Sire. 2009. Loss of teeth and enamel in tetrapods: fossil record, genetic data, and morphological adaptations. *Journal of Anatomy* 214:447-501.

Deméré, T. A., M. R. McGowen, A. Berta, and J. Gatesy. 2008. Morphological and molecular evidence for a stepwise evolutionary transition from teeth to baleen in mysticete whales. *Systematic Biology* 57(1):15-37.

Di Beneditto, A. P. M., and L. R. Monteiro. 2015. Isotopic niche of two coastal dolphins in a tropical marine area: specific and age class comparisons. *Journal of the Marine Biological Association of the United Kingdom* 96:853-858.

Ekdale, E. G., and T. A. Deméré. 2022. Neurovascular evidence for a co-occurrence of teeth and baleen in an Oligocene mysticete and the transition to filter-feeding in baleen whales. Zoological *Journal of the Linnean Society* 194:395-415.

Fahlke, J. M. 2012. Bite marks revisited - evidence for middle-to-late Eocene *Basilosaurus isis* predation on *Dorudon atrox* (both Cetacea, Basilosauridae). *Palaeontologia Electronica* 15:32A.

Fahlke, J. M., K. A. Bastl, G. M. Semprebon, and P. D. Gingerich. 2013. Paleoecology of archaeocete whales throughout the Eocene: dietary adaptations revealed by microwear analysis. *Palaeogeography, Palaeoclimatology, Palaeoecology* 386:690-701.

Fitch, J. E., and R. L. Brownell Jr. 1971. Food habits of the Franciscana *Pontoporia blainvillei* (Cetacea: Platanistidae) from South America. *Bulletin of Marine Science* 21:626-636.

Fitzgerald, E. M. 2006. A bizarre new toothed mysticete (Cetacea) from Australia and the early evolution of baleen whales. *Proceedings of the Royal Society B: Biological Sciences* 273:2955-2963.

Fitzgerald, E. M. G. 2010. The morphology and systematics of Mammalodon colliveri (Cetacea: Mysticeti), a tooth mysticete from the Oligocene of Australia. *Zoological Journal of the Linnean Society* (158):367-476.

Fitzgerald, E. M. G. 2012. Archaeocete-like jaws in a baleen whale. *Biology Letters* 8:94-96.

Fordyce, R. E., and F. G. Marx. 2018. Gigantism precedes filter feeding in baleen whale evolution. *Current Biology* 28:1670-1676.

Galatius, A., R. A. Racicot, M. R. McGowen, and M. T. Olsen. 2020. Evolution and diversification of delphinid skull shapes. *iScience* 23(10):101543.

Geisler, J. H., R. W. Boessenecker, M. Brown, and B. L. Beatty. 2017. The origin of filter feeding in whales. *Current Biology* 27:1-7.

Geisler, J. H., M. W. Colbert, and J. L. Carew. 2014. A new fossil species supports an early origin for toothed whale echolocation. *Nature* 508:383-386.

Geisler, J. H., and A. E. Sanders. 2003. Morphological evidence for the phylogeny of Cetacea. *Journal of Mammalian Evolution* 10:23-129.

Geisler, J. H., and J. M. Theodor. 2009. Hippopotamus and whale ancestry. *Nature* 458:E1-E4.

Guo, Z., and N. Kohno. 2021. A new kentriodontid (Cetacea: Odontoceti) from the early to middle Miocene of the western North Pacific and a revision of kentriodontid phylogeny. *PeerJ* 9:e10945.

Guo, Z., and N. Kohno. 2023. An Early Miocene kentriodontoid (Cetacea: Odontoceti) from the western North Pacific, and its implications for their phylogeny and paleobiogeography. *PLoS ONE* 18:e0280218.

Hall-Aspland, S. A., and T. L. Rogers. 2004. Summer diet of leopard seals (*Hydrurga leptonyx*) in Prydz Bay, Eastern Antarctica. *Polar Biology* 27:729-734.

Harmon, L. J., J. B. Losos, T. Jonathan Davies, R. G. Gillespie, J. L. Gittleman, W. Bryan Jennings, K. H. Kozak, M. A. McPeek, F. Moreno-Roark, T. J. Near, and A. Purvis. 2010. Early bursts of body size and shape evolution are rare in comparative data. *Evolution* 64:2385-2396.

Henning, B., B. de Sá Carvalho, M. M. Pires, M. Bassoi, J. Marigo, C. Bertozzi, and M. S. Araújo. 2017. Geographical and intrapopulation variation in the diet of a threatened marine predator, *Pontoporia blainvillei* (Cetacea). *Biotropica* 50:157-168.

Herrel, A., A. De Smet, L. F. Aguirre, and P. Aerts. 2008. Morphological and mechanical determinants of bite force in bats: do muscles matter? *Journal of Experimental Biology* 211:86-91.

Heyning, J. E. 1989. Comparative facial anatomy of beaked whales (Ziphiidae) and a systematic revision among the families of extant Odontoceti. *Contributions in Science, Natural History Museum of Los Angeles County* 464:1-64.

Heyning, J. E., and J. G. Mead. 1990. Evolution of the nasal anatomy of cetaceans. Pp. 67-79. *In* J. A. Thomas, and R. A. Kastelein, eds. Sensory Abilities of Cetaceans. New York, Springer.

Heyning, J. E., and J. G. Mead. 1996. Suction feeding beaked whales: morphological and observational evidence. *Contributions in Science, Natural History Museum of Los Angeles County* 464:1-12.

Hocking, D. P., A. R. Evans, and E. M. G. Fitzgerald. 2013. Leopard seals (*Hydrurga leptonyx*) use suction and filter feeding when hunting small prey underwater. *Polar Biology* 36:211-222.

Hocking, D. P., F. G. Marx, E. M. G. Fitzgerald, and A. R. Evans. 2017a. Ancient whales did not filter feed with their teeth. *Biology Letters* 13:20170348.

Hocking, D. P., F. G. Marx, T. Park, E. M. G. Fitzgerald, and A. R. Evans. 2017b. A behavioral framework for the evolution of feeding in predatory aquatic mammals. *Proceedings of the Royal Society B*. 284:20162750.

Huggenberger, S., S. Leidenberger, and H. A. Oelschläger. 2017. Asymmetry of the nasofacial skull in toothed whales (Odontoceti). *Journal of Zoology* 302:15-23.

Johnston, C., and A. Berta. 2011. Comparative anatomy and evolutionary history of suction feeding in cetaceans. *Marine Mammal Science* 27:493-513.

Kane, E. A., and C. D. Marshall. 2009. Comparative feeding kinematics and performance of odontocetes: belugas, Pacific white-sided dolphins, and long-finned pilot whales. *Journal of Experimental Biology* 212:3939-3950.

Kaplan, J. D., S. Y. Goodrich, K. Melillo, and D. Reiss. 2019. Behavioural laterality in foraging bottlenose dolphins (*Tursiops truncatus*). *Royal Society Open Science* 6:190929.

Karenina, K., A. Giljov, T. Ivkovich, and V. Malaschichev. 2016. Evidence for the perceptual origin of right-sided feeding biases in cetaceans. *Animal Cognition* 19:239-243.

Kasuya, T., and D. W. Rice. 1970. Notes on baleen whale plates and arrangement of parasitic barnacles on gray whales. *Scientific Reports of the Whales Research Institute*, Tokyo 22:39-43.

Kienle, S. S., C. J. Law, D. P. Costa, A. Berta, and R. S. Mehta. 2017. Revisiting the behavioural framework of feeding in predatory aquatic mammals. *Proceedings of the Royal Society B*. 284:20171035.

Kimura, T., and Y. Hasegawa. 2019. A new species of *Kentriodon* (Cetacea, Odontoceti, Kentriodontidae) from the Miocene of Japan. *Journal of Vertebrate Paleontology* 39:e1566739.

Lambert, O., G. Bianucci, and B. L. Beatty. 2014. Bony outgrowths on the jaws of an extinct sperm whale support macroraptorial feeding in stem physeteroids. *Naturwissenschaften* 101:517-521.

Lambert, O., G. Bianucci, K. Post, C. Muizon, R. Salas-Gismondi, M. Urbina, and J. Reumer. 2010. The giant bite of a new raptorial sperm whale from the Miocene epoch of Peru. *Nature* 466:105-108.

Lambert, O., G. Bianucci, M. Urbina, and J. H. Geisler. 2017. A new inioid (Cetacea, Odontoceti, Delphinida) from the Miocene of Peru and the origin of modern dolphin and porpoise families. *Zoological Journal of the Linnean Society* 179(4):919-946.

Lambert, O., and C. De Muizon. 2013. A new long-snouted species of the Miocene pontoporiid dolphin Brachydelphis and a review of Mio-Pliocene marine mammal levels in the Sacaco Basin, Peru. *Journal of Vertebrate Paleontology* 33:709-721.

Lambert, O., S. J. Godfrey, and E. M. G. Fitzgerald. 2019. *Yaquinacetus meadi,* a new latest Oligocene-Early Miocene dolphin (Cetacea, Odontoceti, Squaloziphiidae, Fam. nov.) from the Nye Mudstone (Oregon, U.S.A.). *Journal of Vertebrate Paleontology* 38:1-19.

Lloyd, G. T., and G. J. Slater. 2021. A total-group phylogenetic metatree for Cetacea and the importance of fossil data in diversification analyses. *Systematic Biology* 70(5):922-939.

Loch, C., J. A. Kieser, and R. E. Fordyce. 2015. Enamel ultrastructure in fossil cetaceans (Cetacea: Archaeoceti and Odontoceti). *PLoS ONE* 10:e0116557.

Lowry, L. F., J. W. Testa, and W. Calvert. 1988. Notes on winter feeding of crabeater and leopard seals near the Antarctic Peninsula. *Polar Biology* 8:475-478.

Macleod, C. D., J. S. Reidenberg, M. Weller, M. B. Santos, J. Herman, J. Goold, and G. J. Pierce. 2007. Breaking symmetry: the marine *environment, prey size, and the evolution of asymmetry in cetacean skulls. The* Anatomical Record 290:539-545.

MacNeilage, P. F. 2013. Vertebrate whole-body action asymmetries and the evolution of right handedness: a comparison between humans and marine mammals. *Developmental Psychobiology* 55:577-587.

Martins, M. C. I., T. Park, R. A. Racicot, and N. Cooper. 2020. Intraspecific variation in the cochlea of harbour porpoises (*Phocoena phocoena*) and its implications for comparative studies across odontocetes. *PeerJ* 8:e8916.

Marx, F. G., and R. E. Fordyce. 2015. Baleen boom and bust: a synthesis of mysticete phylogeny, diversity, and disparity. *Royal Society Open Science* 2(4):140434.

Marx, F. G., D. P. Hocking, T. Park, T. Ziegler, A. R. Evans, and E. M. G. Fitzgerald. 2016a. Suction feeding preceded filtering in baleen whale evolution. Memoirs of Museum Victoria 75:71-82.

Marx, F. G., O. Lambert, and M. D. Uhen. 2016b. Cetacean Paleobiology. John Wiley & Sons, Chichester, UK.

Marx, F. G., C. H. Tsai, and R. E. Fordyce. 2015. A new Early Oligocene toothed "baleen" whale (Mysticeti: Aetiocetidae) from western North America: one of the oldest and smallest. Royal Society Open Science 2:150476.

McCurry, M. R., A. R. Evans, E. M. G. Fitzgerald, J. W. Adams, P. D. Clausen, and C. R. McHenry. 2017a. The remarkable convergence of skull shape in crocodilians and toothed whales. *Proceeding of the Royal Society B: Biological Sciences* 284:20162348.

McCurry, M. R., E. M. G. Fitzgerald, A. R. Evans, J. W. Adams, and C. R. McHenry. 2017b. Skull shape reflects prey size niche in toothed whales. *Biological Journal of the Linnean Society* 121:936-946.

McCurry, M. R., and N. Pyenson. 2019. Hyper-longirostry and kinematic disparity in extinct toothed whales. *Paleobiology* 45:21-29.

McGowen, M. R. 2011. Towards the resolution of an explosive radiation - A multilocus phylogeny of oceanic dolphins (Delphinidae). *Molecular Phylogenetics and Evolution* 60:345-357.

McGowen, M. R., G. Tsagkogeorga, S. Álvarez-Carretero, M. Dos Reis, M. Struebig, R. Deaville, P. D. Jepson, S. Jarman, A. Polanowski, P. A. Morin, and S. J. Rossiter. 2020. Phylogenomic resolution of the Cetacean tree of life using target sequence capture. *Systematic Biology* 69(3):479-501.

Mead, J. G. 1975. Anatomy of the external nasal passages and facial complex in the Delphinidae (Mammalia: Cetacea). *Smithsonian Contributions to Zoology* 207:1-72.

Miller, G. S. J. 1923. The telescoping of the cetacean skull. *Smithsonian Miscellaneous Collections* 76(5):1-71.

Muizon, C. 1988. Les relations phylogénétiques des Delphinida (Cetacea, Mammalia). *Annales de Paleontologie* 74:159-227

Muizon, C. 1988. Les vertébrés fossiles de la Formation Pisco (Pérou). Troisiéme partie: Les Odontocétes (Cetacea, Mammalia) du Miocéne. *Travaux de I'Institut Francais d'Etudes Andines* 78:1-244

Muizon, C. 1993. Walrus-like feeding adaptation in a new cetacean from the Pliocene of Peru. *Nature* 365:745-748.

Muizon, C., and D. P. Domning. 2002. The anatomy of Odobenocetops (Delphinoidea, Mammalia), the walrus-like dolphin from the Pliocene of Peru and its palaeobiological implications. *Zoological Journal of the Linnean Society* 134:423-452.

Mutha, P. K., K. Y. Haaland, and R. L. Sainburg. 2012. The efects of brain lateralization on motor control and adaptation. *Journal of Motor Behavior* 44:455-469.

Ness, A. R. 1967. A measure of asymmetry of the skulls of odontocete whales. *Journal of Zoology* 153(2):209-221.

Oelschläger, H. A. 1990. Evolutionary morphology and acoustics in the dolphin skull. Pp. 137-162. *In* J. A. Thomas, and R. A. Kastelein, eds. Sensory Abilities of Cetaceans. Plenum Press, New York.

Øritsland, T. 1977. Food consumption of seals in the Antarctic pack ice. Pp. 749-768. *In* G. A. Llano, ed. Adaptations within antarctic ecosystems, Proceedings of the THird SCAT symposium on Antarctic Biology. Smithsonian Institution, Washington D.C.

Pagel, M. 1999. Inferring the historical patterns of biological evolution. *Nature* 401:877-884.

Paradis, E., J. Claude, and K. Strimmer. 2004. APE: analyses of phylogenetics and evolution in R language. *Bioinformatics* 20(2):289-290.

Park, T., E. M. G. Fitzgerald, and A. R. Evans. 2016. Ultrasonic hearing and echolocation in the earliest toothed whales. *Biology Letters* 12:20160060.

Pauly, D., A. W. Trites, E. Capuli, and V. Christensen. 1998. Diet composition and trophic levels of marine mammals. *ICES Journal of Marine Science* 55:467-481.

Peredo, C. M., J. S. Peredo, and N. Pyenson. 2018a. Convergence on dental simplification in the evolution of whales. *Paleobiology* 44:434-443

Peredo, C. M., N. D. Pyenson, C. D. Marshall, and M. D. Uhen. 2018b. Tooth loss precedes the origin of baleen in whales. *Current Biology* 28:3992-4000.

Peredo, C. M., M. D. Uhen, and D. M. Nelson. 2018c. A new kentriodontid (Cetacea: Odontoceti) from the early Miocene Astoria Formation and a revision of the stem delphinidan family Kentriodontidae. *Journal of Vertebrate Paleontology* 38:e1411357

Peri, E., P. L. Falkingham, A. Collareta, and G. Bianucci. 2022. Biting in the Miocene seas: estimation of the bite force of the macroraptorial sperm whale *Zygophyseter varolai* using finite element analysis. *Historical Biology* 34:1916-1927.

Perrin, W. F. 1975. Variation of spotted and spinner porpoise (genus *Stenella*) from the Eastern Pacific and Hawaii. *Bulletin of the Scripps Institution of Oceanography* 21:1-204.

Perrin, W. F., B. Würsig, and J. M. G. Thewissen, eds. 2009. Encyclopedia of Marine Mammals. Academic Press, San Diego CA.

Pitman, R. L., and J. Durban. 2012. Coopearative hunting behavior, prey selectivity, and prey handling by pack ice killer whales (*Orcinus orca*), type B, in Antarctic Peninsula waters. *Marine Mammal Science* 28:16-36.

Post, K., S. Louwye, and O. Lambert. 2017. Scaldiporia vandokkumi, a new pontoporiid (Mammalia, Cetacea, Odontoceti) from the Late Miocene to earliest Pliocene of the Westerschelde estuary (The Netherlands). *PeerJ* 5:e3991.

Racicot, R. A., T. A. Deméré, B. L. Beatty, and R. W. Boessenecker. 2014. Unique feeding morphology in a new prognathous extinct porpoise from the Pliocene of California. *Current Biology* 24(7):774-779.

Racicot, R. A., and T. Rowe. 2014. Endocranial anatomy of a new fossil porpoise (Odontoceti, Phocoenidae) from the Pliocene San Diego Formation of California. *Journal of Vertebrate Paleontology* 88:652-663.

Rauschmann, M. A., S. Huggenberger, L. S. Kossatz, and H. A. Oelschläger. 2006. Head morphology in perinatal dolpins: a window into phylogeny and ontogeny. *Journal of Morphology* 267:1295-1315.

Revell, L. J. 2012. Phytools: an R package for phylogenetic comparative biology (and other things). *Methods in Ecology and Evolution* 3:217-223.

Rodríguez, D., L. Rivero, and R. Bastida. 2002. Feeding ecology of the Franciscana (*Pontoporia blainvillei*) in marine and estuarine waters of Argentina. *Latin American Journal of Aquatic Mammals Special Issue* 1:77-94.

Roe, L. J., J. G. M. Thewissen, J. Quade, J. R. O'Neil, S. Bajpai, A. Sahni, and S. T. Hussain. 1998. Isotopic approaches to understanding the terrestrial-to-marine transition of the earliest cetaceans. *In* J. G. M. Thewissen, ed. The Emergence of Whales. Plenum Press, New York.

Roston, R. A., and V. L. Roth. 2019. Cetacean skull telescoping brings evolution of cranial sutures into focus. *The Anatomical Record* 302:1055-1073.

Sanders, A. E., and L. G. Barnes. 2002. Paleontology of the Late Oligocene Ashley and Chandler Bridge Formations of South Carolina, 3: Eomysticetidae, a new family of primitive mysticetes (Mammalia: Cetacea). *Smithsonian Contributions to Paleobiology* 93:313-356.

Siniff, D. B., and S. Stone. 1985. The role of the leopard seal in the tropho-dynamics of the Antarctic marine ecosystem. Pp. 555-560. *In* W. R. Siegfried, P. R. Condy, and R. M. Laws, eds. Antarctic nutrient cycles and food webs. Springer, Berlin.

Snively, E., J. M. Fahlke, and R. C. Welsh. 2015. Bone-breaking bite force of *Basilosaurus isis* (Mammalia, Cetacea) from the Late Eocene of Egypt estimated by finite element analysis. *PLoS ONE* 10:e0118380.

Swift, C. C., and L. G. Barnes. 1996. Stomach contents of *Basilosaurus cetoides:* implications for the evolution of cetacean feeding behavior and the evidence of vertebrate fauna of epicontintal Eocene seas. *The Paleontological Society Special Publication* 8:380.

Takeuchi, H., Matsuishi, T.F., and Hayakawa, T. 2024. A tradeoff evolution between acoustic fat bodies and skull muscles in toothed whales. *Gene* 901:148167.

Tellechea, J. S., W. Perez, D. Olsson, M. Lima, and W. Norbis. 2017. Feeding habits of Franciscana dolphins (Pontoporia blainvillei): echolocation or passive listening? *Aquatic Mammals* 43:430-438.

Thewissen, J. G. M., L. N. Cooper, M. T. Clementz, S. Bajpai, and B. N. Tiwari. 2007. Whales originated from aquatic artiodactyls in the Eocene epoch of India. *Nature* 450:1190-1193.

Thewissen, J. G. M., J. D. Sensor, M. T. Clementz, and S. Bajpai. 2011. Evolution of dental wear and diet during the origin of whales. *Paleobiology* 37(4):655-669.

Troina, G. C., S. Botta, E. R. Secchi, and F. Dehairs. 2016. Ontogenetic and sexual characterization of the feeding habits of franciscanas, Pontoporia blainvillei, based on tooth dentin carbon and nitrogen stable isotopes. *Marine Mammal Science* 32:1115-1137.

Turnbull, W. D. 1970. The mammalian masticatory apparatus. Fieldiana Geology 18:149-356.

Uhen, M. D. 2004. Form, function, and anatomy of *Dorudon atrox* (Mammalia, Cetacea): an archaeocete from the Middle to Late Eocene of Egypt. *University of Michigan Papers on Paleontology* 34:1-222.

Vélez-Juarbe, J. 2017. A new stem odontocete from the late Oligocene Pysht Formation in Washington State, U.S.A. *Journal of Vertebrate Paleontology* 37:e1366916.

Viola, M. N. P., L. Riccialdelli, M. F. Negri, M. V. Panebianco, H. O. Panarello, and H. L. Cappozzo. 2017. Intra-specific isotope variations of franciscana dolphin Pontoporia blainvillei regarding biological parameters and distinct environment. *Mammalian Biology* 85:47-54.

Werth, A. J. 2000. Feeding in marine mammals. Pp. 487-526. *In* K. Schwenk, ed. Feeding: Form, Function, and Evolution in Tetrapod Vertebrates. Academic Press, San Diego.

Werth, A. J. 2006. Mandibular and dental variation and the evolution of suction feeding in Odontoceti. *Journal of Mammalogy* 87(3):579-588.

Werth, A. J., and B. L. Beatty. 2023. Osteological correlates of evolutionary transitions in cetacean feeding and related oropharyngeal functions. *Frontiers in Ecology and Evolution* 11:311.

Appendix 1. List of included taxa and specimens

Taxonomic Group	Species	Specimen(s)
Archaeocete	*Aegytocetus tarfa*	MSNT UP I-15459
Archaeocete	*Ambulocetus natans*	MSNT UP I-16826
Archaeocete	*Basilosaurus isis*	SMNS 11787
Archaeocete	*Cynthiacetus peruvianus*	MNHN.F.PRU10_cast
Archaeocete	*Dorudon atrox*	UMMP 118139
Archaeocete	*Zygorhiza kochi*	USNM 11962
Mysticeti	*Aetiocetus cotylalveus*	USNM 25210
Mysticeti	*Coronodon havensteini*	CCNHM 108
Mysticeti	*Fucaia goedertorum*	LACM 131146
Mysticeti	*Janjucetus hunderi*	NMV P216929_cast
Xenorophidae	*Albertocetus meffordorum*	CCNHM 218, CCNHM 303.1
Xenorophidae	*Cotylocara macei*	CCNHM 101
Xenorophidae	*Xenorophus simplicidens*	CCNHM 104.1, CCNHM 168, ChM PV4823, ChM PV5022
Stem Odontocete	*Agorophius pygmaeus*	CCNHM 624
Stem Odontocete	*Ankylorhiza tiedmani*	CCNHM 103
Stem Odontocete	*Argyrocetus joaquinensis*	USNM 11996
Stem Odontocete	*Eosqualodon n. sp.*	CCNHM 170.1
Stem Odontocete	*Prosqualodon davidis*	USNM 467596
Stem Odontocete	*Squaloziphius emlongi*	USNM 181528
Stem Odontocete	*Waipatia maerwhenua*	OU 22095_cast
Physeteroidea	*Kogia breviceps*	USNM 22015, USNM 243857, USNM 283625
Physeteroidea	*Kogia sima*	NHM.1952.8.28.1
Physeteroidea	*Livyatan melvillei*	MSNT UP
Physeteroidea	*Physeter macrocephalus*	NHMUK ZD 2007.100
Platanistoidea	*Eurhinodelphis longirostris*	USNM 244404
Platanistoidea	*Notocetus vanbenedeni*	AMNH F9485
Platanistoidea	*Platanista gangetica*	AMNH 8461, USNM 172409
Platanistoidea	*Schizodelphis barnesi*	MNHN AMN 19
Platanistoidea	*Zarhachis flagellator*	USNM 10911
Platanistoidea	*Zarhinocetus errabundus*	LACM 149588
Ziphiodea	*Berardius arnuxii*	NHM 1935.10.23.1
Ziphiodea	*Berardius bairdi*	NHM 1954.9.21.1, USNM 550895
Ziphiodea	*Hyperoodon ampullatus*	NHM UK ZD 1992.42
Ziphiodea	*Hyperoodon planifrons*	NHM 1952.9.30.1
Ziphiodea	*Mesoplodon bidens*	USNM 504146, USNM 572996, USNM 593438
Ziphiodea	*Mesoplodon carlhubbsi*	USNM 504128
Ziphiodea	*Mesoplodon densirostris*	ChM CM434
Ziphiodea	*Mesoplodon europaeus*	USNM 504256, USNM 571665, USNM 593437
Ziphiodea	*Mesoplodon ginkgodens*	USNM 298237
Ziphiodea	*Mesoplodon grayi*	NHM 1952.7.21.1, USNM 49880, USNM 550149
Ziphiodea	*Mesoplodon hectori*	NHM 1949.8.19.1

Appendix 1. List of included taxa and specimens, continued

Ziphiodea	*Mesoplodon hotaula*	USNM 593426
Ziphiodea	*Mesoplodon layardi*	USNM 550150
Ziphiodea	*Mesoplodon mirus*	USNM 504612
Ziphiodea	*Mesoplodon perrini*	USNM 504260
Ziphiodea	*Mesoplodon peruvianus*	USNM 571257, USNM 571258
Ziphiodea	*Mesoplodon stejnegeri*	UAM 24066, USNM 504330, USNM 504331, USNM 504865
Ziphiodea	*Messapicetus longirostris*	MSNT UP
Ziphiodea	*Tasmacetus shepherdi*	USNM 484878
Ziphiodea	*Ziphius cavirostris*	NHM 2006.15, NHM UK 1915.7.20.1, UAM 83269, USNM 550734, USNM 594597
Inioidea	*Brachydelphis mazeazi*	MNHN.F.PPI 266
Inioidea	*Inia geoffrensis*	USNM 49582, USNM 93415, USNM 239667, USNM 395415
Inioidea	*Lipotes vexillifer*	AMNH 57333
Inioidea	*Parapontoporia sternbergi*	SDSNH 75060, SDSNH 226633
Inioidea	*Pliopontos littoralis*	MNHN SAS 193
Inioidea	*Pontoporia blainvillei*	USNM 482727, USNM 482763, USNM 482771
Delphinoidea	*Atocetus iquensis*	MNHN.F.PPI 113
Delphinoidea	*Cephalorhynchus commersoni*	USNM 252568, USNM 550156, USNM 550449
Delphinoidea	*Cephalorhynchus eutropia*	NHM 1881.8.17.1, USNM 21167, USNM 395374, USNM 395375
Delphinoidea	*Cephalorhynchus heavisidii*	NHM 1948.7.27.1, USNM 550067
Delphinoidea	*Cephalorhynchus hectori*	USNM 84588, USNM 500864
Delphinoidea	*Delphinapterus leucas*	USNM 305071
Delphinoidea	*Delphinus delphis*	AMNH 176, AMNH 34277, AMNH 35401, AMNH 75332, AMNH 77931, AMNH 121098, AMNH 130119, AMNH 130217, AMNH 135506, AMNH 143517, AMNH 143518, AMNH 180668, AMNH 180670, AMNH 239124, AMNH 239125, AMNH 239126, AMNH 239128, AMNH 239129, AMNH 239131, AMNH 239133, AMNH 239134, AMNH 239135, AMNH 239136, AMNH 239137, AMNH 239138, AMNH 239139, AMNH 239140, AMNH 239141, AMNH 239142, AMNH 239143, AMNH 239144, AMNH 239146, AMNH 239147, AMNH 239148, AMNH 239149, AMNH 239151, DUNUC 1961, USNM 22881
Delphinoidea	*Feresa attenuata*	USNM 504916, USNM 504917, USNM 504918
Delphinoidea	*Globicephala macrorhynchus*	NHM 1912.10.27.1
Delphinoidea	*Globicephala melas*	AMNH 34934, AMNH 235593, AMNH 235597
Delphinoidea	*Grampus griseus*	USNM 24224, USNM 500271, USNM 571602
Delphinoidea	*Kentriodon pernix*	USNM 10670
Delphinoidea	*Lagenodelphis hosei*	USNM 504411, USNM 571619, USNM 594200
Delphinoidea	*Lagenorhynchus albirostris*	AMNH 37162, AMNH 143520
Delphinoidea	*Lamprolithax simulans*	LACM 37858
Delphinoidea	*Leucopleurus acutus*	AMNH 37161, AMNH 143513, USNM 504196
Delphinoidea	*Lissodelphis borealis*	USNM 550026, USNM 550027, USNM 550188
Delphinoidea	*Lomacetus ginsburgi*	MNHN.F.PPI 104
Delphinoidea	*Monodon monoceros*	AMNH 73316, USNM 267959, USNM 267960

Appendix 1. List of included taxa and specimens, continued

Delphinoidea	*Neophocaena asiaeorientalis*	DNHM 20697, USNM 240001, USNM 240002
Delphinoidea	*Neophocaena phocaenoides*	NHM 1903.9.12.3
Delphinoidea	*Odobenocetops peruvianus*	SMNS PAL 2491
Delphinoidea	*Orcaella brevirostris*	NHM 1883.11.20.2
Delphinoidea	*Orcaella heinsohni*	USNM 284430
Delphinoidea	*Orcinus orca*	USNM 11980
Delphinoidea	*Peponocephala electra*	USNM 504510, USNM 504511
Delphinoidea	*Phocoena dioptrica*	NHM 1939.9.30.1, USNM 571486
Delphinoidea	*Phocoena phocoena*	AMNH 10188, AMNH 10200, AMNH 77929, AMNH 212161
Delphinoidea	*Phocoena spinipinnis*	USNM 395753, USNM 550139, USNM 550229, USNM 550287
Delphinoidea	*Phocoenoides dalli*	USNM 238083, USNM 276062, USNM 276394
Delphinoidea	*Piscolithax longirostris*	MNHN SAS 933
Delphinoidea	*Pseudorca crassidens*	AMNH 99681, USNM 11320, USNM 218360
Delphinoidea	*Sagmatias australis*	NHM 1944.11.30.1, USNM 395344, USNM 395345, USNM 395348
Delphinoidea	*Sagmatias cruciger*	AMNH 35150
Delphinoidea	*Sagmatias obliquidens*	USNM 290642, USNM 290644, USNM 290646
Delphinoidea	*Sagmatias obscurus*	NHM 1846.3.11.8, USNM 550742, USNM 550743, USNM 550757
Delphinoidea	*Semirostrum cerutti*	SDSNH 65276
Delphinoidea	*Sotalia fluviatillis*	AMNH 92203, AMNH 94169
Delphinoidea	*Sotalia guianensis*	USNM 571558
Delphinoidea	*Sousa chinensis*	NHM 1992.97
Delphinoidea	*Sousa plumbea*	USNM 550939, USNM 550941
Delphinoidea	*Sousa sahulensis*	NHM 1992.92
Delphinoidea	*Sousa teuszii*	NHM 1992.138
Delphinoidea	*Stenella attenuata*	AMNH 180559, NHM 1966.11.18.5, USNM 395333, USNM 395334, USNM 395336
Delphinoidea	*Stenella clymene*	AMNH 239115, USNM 550531, USNM 550532, USNM 550534
Delphinoidea	*Stenella coeruleoalba*	AMNH 177, AMNH 80274, SDNHM 13958, SDNHM 23579, USNM 571260, USNM 571561, USNM 571580
Delphinoidea	*Stenella frontalis*	AMNH 239111, AMNH 239117, USNM 550024, USNM 550025, USNM 550355
Delphinoidea	*Stenella longistrostris*	NHM 1966.11.1.4, USNM 395269, USNM 395270, USNM 395271
Delphinoidea	*Steno bredanesis*	USNM 572789, USNM 572790, USNM 572795
Delphinoidea	*Tursiops aduncus*	NHM 1882.1.2.3
Delphinoidea	*Tursiops truncatus*	ChM CM256, SDNHM 11102, SDNHM 20143, SDNHM 21212, SDNHM 23798, USNM 571698